

**Roles of Antibody in Vaccine-Elicited Protection Against Virulent *Francisella tularensis*
Aerosolized Infection**

by

Emily L. Olsen

BS, The University of Alabama in Huntsville, 2018

Submitted to the Graduate Faculty of the
Department of Infectious Diseases and Microbiology
Graduate School of Public Health in partial fulfillment
of the requirements for the degree of
Master of Science

University of Pittsburgh

2020

UNIVERSITY OF PITTSBURGH
GRADUATE SCHOOL OF PUBLIC HEALTH

This thesis was presented

by

Emily L. Olsen

It was defended on

April 1, 2020

and approved by

Simon Barratt-Boyes BVSc, PhD, DACVIM
Professor
Department of Infectious Diseases and Microbiology
Graduate School of Public Health
University of Pittsburgh

Joshua T. Mattila, PhD
Assistant Professor
Department of Infectious Diseases and Microbiology
Graduate School of Public Health
University of Pittsburgh

Thesis Advisor:
Douglas Reed, PhD
Associate Professor
Department of Immunology
School of Medicine
Associate Professor
Department of Infectious Diseases and Microbiology
Graduate School of Public Health
University of Pittsburgh

Copyright © by Emily L. Olsen

2020

Roles of Antibody in Vaccine-Elicited Protection Against Virulent *Francisella tularensis* Aerosolized Infection

Emily L. Olsen, MS

University of Pittsburgh, 2020

Abstract

Francisella tularensis, the causative agent of tularemia, is a facultative intracellular bacterium that infects a wide variety of cell types, most notably phagocytes. Initial studies of *F. tularensis* focused on using plasma to passively immunize subjects as a mechanism of protection, with varied results. Here, we purified the antibodies from plasma of rabbits that were immunized in a prime-boost schedule of a live attenuated mutant of virulent *Ft. tularensis* (Schu S4 Δ AroD) infection that also survived challenge from the fully virulent strain. We also examined the ability of the antibodies to opsonize and fix complement to *Ft. holarctica* Live Vaccine Strain. When BALB/c mice were passively immunized either intraperitoneally or intranasally with our polyclonal antibody solutions there was an extension of time to death in lethal doses, significantly less weight loss in immunized animals, and a slight decrease in bacterial titers within the tissues of animals. These data indicate that while antibodies alone are not a mechanism of protection in the mouse model, they do reduce clinical disease and may play a role in vaccine-mediated protection against aerosolized infection with the Live Vaccine Strain. These findings further warrant future studies in other animal models that recapitulate human disease. These findings contribute to the development of therapeutics for infection, and are significant to public health because of the potential of *F. tularensis* to be used as a biological weapon.

Table of Contents

Preface.....	xii
1.0 Introduction.....	1
1.1 <i>Francisella tularensis</i> Disease and Epidemiology	2
1.1.1 Routes of Infection, Clinical Disease, Epidemiology	2
1.1.1.1 Focus on Aerosol Infections	3
1.1.2 Epidemiology of Natural <i>Francisella</i> Infection	3
1.2 Immune Response to <i>Francisella tularensis</i> and Current Vaccine Strategies	5
1.2.1 <i>Francisella tularensis</i> Pathogenesis and Host Response.....	5
1.2.2 Vaccine Strategies	6
1.3 Humoral Immunity in <i>F. tularensis</i> Infections	7
1.3.1 Passive Immunization and Therapeutics	11
1.4 Working with <i>Francisella tularensis</i> in the Laboratory Setting.....	12
1.4.1 Biosafety	12
1.4.2 Animal Models for <i>Francisella</i> Infections.....	12
1.5 Public Health Significance	13
2.0 Specific Aims	15
2.1 Aim 1: Purify and Characterize Antibodies Produced from Hyperimmune Rabbit Plasma.....	15
2.2 Aim 2: Examine the Potential Role of Antibodies in Protection Elicited by Vaccination.....	16
3.0 Materials and Methods.....	17

3.1 Animal Models Used and Biosafety	17
3.2 Antibody Purification.....	17
3.2.1 Optimization of Purification of Antibody	18
3.3 SDS Gel Analysis	18
3.4 Enzyme-linked Immunosorbent Assay (ELISA) Analysis.....	19
3.5 Bicinchoninic Acid (BCA) Assays	20
3.6 Cell Culture.....	20
3.7 Bacterial Methods and Culture.....	21
3.7.1 Determining Aerosol Dose of RML LVS	21
3.8 LVS Infection of J774 Macrophages.....	23
3.9 Opsonization of LVS	24
3.10 Complement Fixation of RML LVS	24
3.11 Agglutination Tests of RML LVS	25
3.12 LD50 Determination of RML LVS in Aerosol Infection of BALB/c Mice	26
3.13 Antibody Passive Immunization and Subsequent Challenge with Aerosolized RML LVS	27
4.0 Results	29
4.1 Characterization of Immune Plasma from NZW Rabbit Survivors of SCHU S4 ΔaroD Prime/Boost Vaccination and SchuS4 Challenge	29
4.1.1 SDS Gel Purification.....	29
4.1.2 ELISA Analysis	31
4.1.3 BCA Assays.....	33
4.2 Effects of Antibodies on RML LVS	37

4.2.1 Opsonization	37
4.2.2 Agglutination Tests	38
4.2.3 Infection Assays of J774s	39
4.3 Passive Protection from Lethal RML LVS Aerosol Infection in BALB/c Mice	42
4.3.1 Determining LD50 of RML LVS in Aerosol Infection of BALB/c Mice	42
4.3.1.1 Aerosol Dose	42
4.3.1.2 Survival Curve of BALB/c Mice.....	43
4.3.1.3 Clinical Signs of Disease in BALB/c Mice	44
4.3.2 Comparison between Treatment Routes.....	45
4.3.2.1 Aerosol Dose	45
4.3.2.2 Survival Curve of BALB/c Mice.....	45
4.3.2.3 Weight Loss of BALB/c Mice.....	47
4.3.2.4 Tissue-Specific Bacterial Burden in BALB/c Mice.....	48
4.3.3 High-Dose Challenges	49
4.3.3.1 Aerosol Dose	49
4.3.3.2 Survival Curve of BALB/c Mice.....	50
4.3.3.3 Weight Loss of BALB/c Mice.....	51
4.3.3.4 Tissue-Specific Bacterial Burden in BALB/c Mice.....	53
5.0 Discussion.....	54
5.1 Plasma Purification	54
5.2 In vitro Effects of Antibody on <i>F. tularensis</i> RML LVS.....	55
5.3 Passive Immunization of BALB/c Mice Against Aerosolized RML LVS.....	57
5.4 Importance	59

Appendix Supplemental Tables and Figures..... 61
Bibliography 65

List of Tables

Table 1. Summary of Literature Examining Passive Protection Against <i>F. tularensis</i>.....	10
Table 2. Protein Concentrations from Optimizing Plasma Purification.	33
Table 3. Protein Concentrations from Hyperimmune Rabbit Plasma Purification.	34
Table 4. Protein Concentrations from Naive Rabbit Plasma.	35
Table 5. Agglutination Titers of Hyperimmune and Non-Immune Antibodies.....	38
Table 6. Aerosol Summary for LD50 Determination	42
Table 7: Aerosol Summary for Determining Passive Immunization Route.....	45
Table 8. Aerosol Summary for High-Dose RML LVS Challenge in Mice - Trial 1.....	49
Table 9. Aerosol Summary for High-Dose RML LVS Challenge in Mice - Trial 2.....	49
Table 10. ELISA Values of Optimization of Plasma Purification.....	62
Table 11. ELISA Values of Hyperimmune Plasma Purification Products.....	62
Table 12. ELISA Values of Naïve Rabbit Plasma Purification Products.....	62

List of Figures

Figure 1 Global distribution of all subspecies of <i>F. tularensis</i>.....	4
Figure 2 U.S. Cases of Tularema in 2018.....	4
Figure 3. Schematic diagram of IgG.	8
Figure 4. Timeline schematic of BALB/c experiment.....	28
Figure 5. SDS gel analysis of immune plasma purification.....	29
Figure 6. SDS gel to assess purity during each step of the immunoglobulin purification process.....	30
Figure 7. ELISA of immune plasma purification products.	31
Figure 8. ELISA of Products from Hyperimmune Rabbit Plasma Purification.....	32
Figure 9. ELISA of products from naive rabbit plasma.	33
Figure 10. BCA Standard Curve for Optimization Products.	34
Figure 11. BCA Standard Curve for Hyperimmune Purification Products.	35
Figure 12. BCA Standard Curve for Naïve Rabbit Plasma Purification.	36
Figure 13. Incubation of immune antibodies and <i>F. tularensis</i> RML LVS result in lower bacterial titers.....	37
Figure 14. Complement-Mediated Killing of RML LVS with Antibodies.	38
Figure 15. Comparison of AT C LVS strain and RML LVS straing during infection of J774 cells.	40
Figure 16. Effects of opsonization of RML LVS during infection with J774 cells.....	41
Figure 17. Survival of BALB/c mice with varying doses of aerosolized RML LVS.	43

Figure 18. (A) Weight Loss and (B) Clinical Score of BALB/c Mice Infected with Different Doses of RML LVS.	44
Figure 19. Survival Curve of BALB/c Mice Passively Immunized Either i.n. or i.p.	45
Figure 20. Weight Loss of BALB/c Mice Immunized via Different Routes.	47
Figure 21. Bacterial Titers in the Lungs, Livers, and Spleens of BALB/c Mice Passively Immunized i.p. or i.n.	48
Figure 22. Survival Curve of Passively Immunized BALB/c Mice Challenged with RML LVS – Trial 1.	50
Figure 23. Survival Curve of Passively Immunized BALB/c Mice Challenged with RML LVS – Trial 2.	50
Figure 24. Weight Weight Loss of BALB/c Mice after Aerosol Challenge, (A) Over Time and (B) on Day 4 Post Infection.	51
Figure 25. Weight loss of passively immunized BALB/c mice after high-dose aerosol challenge of RMS LVS.	52
Figure 26. Bacterial burden in immunized BALB/c mice challenged with high-dose RML LVS.	53
Figure 27. Infection Assay Schematic	61
Figure 28. Purification of Antibody Schematic.	61
Figure 29. Agglutination Schematic Showing Antibody and Antigen Dilutions.	63
Figure 30. Survival of i.n. Treated Mice Only.	63
Figure 31. Survival of i.p. Treated Mice Only.	64

Preface

I would like to thank all members of the Reed lab in helping perform these experiments and for the endless amounts of advice given to me in order to become successful. I would like to thank Jen Bowling in helping me with initial mouse studies and infection assays and Katie Willett for the continued support and help with ELISAs and animal studies. I would also like to thank both Summer Xia and Katie Willett for the willingness to always help with animal work and perform wellness checks so that I could work on other components of this project. Finally, I would like to thank all members of my committee for the advice given to me to be a better scientist and to never give up in trying to find answers in my results.

1.0 Introduction

Francisella tularensis, the causative agent of tularemia, is a gram-negative coccobacillus that establishes infection extracellularly and intracellularly in a wide range of cells. It was originally discovered in 1911 by George McCoy while investigating an outbreak of what was believed to be plague in ground squirrels (1) in Tulare County, California, subsequently naming the agent *Bacterium tularense*. Two years later, Edward Francis determined that the outbreak of “deer fly fever” in the Midwest and later the common “rabbit fever” butchers developed from processing infectious rabbits were both caused by the same organism, naming the condition tularemia. The name of bacterium was later changed to *Francisella tularensis* in his honor (1). There are currently four subspecies of *F. tularensis*: *tularensis* (type A), *holarctica* (type B), *novicida*, and *mediasiatica*. Of these, subspecies *tularensis* is the most virulent and is primarily found in the United States. Type B is more common than type A and primarily seen in both the United States and Europe. All subspecies are almost exclusively seen in the Northern Hemisphere (2). Subspecies *mediasiatica* and *novicida* are not known to cause disease in humans who are immunocompetent.

Currently, there is no vaccine licensed for use in the United States, although there is an attenuated strain “Live Vaccine Strain” (LVS) that is used as investigational new drug to some at-risk personnel (3). This strain was originally developed from a *Ft holarctica* strain by the USSR and was attenuated through serial passage before being gifted to the United States. The exact mechanisms of attenuation in humans are unknown, leading to concerns of spontaneous reversion. In this study, we use the Rocky Mountain Labs (RML) LVS strain. This strain is reported to be more virulent than the commercial LVS biovar (ATCC LVS) (4).

1.1 *Francisella tularensis* Disease and Epidemiology

1.1.1 Routes of Infection, Clinical Disease, Epidemiology

The symptoms and severity of infections with *F. tularensis* vary by subspecies and route of entry (5). The most common natural source of infection is through tick bites and contact with infected animals such as mice, deer, or rabbits. This often produces the ulceroglandular or glandular form of disease, which is characterized by an ulcer forming at the site of infection as well as lymphadenopathy, malaise, fever, chills, and other signs of generalized febrile illness. The glandular form of disease lacks an ulcer but is otherwise comparable. If the bacteria are present in contaminated food, the resulting disease, the oropharyngeal form, often portrays as ulcers along the mucus membranes as well as tonsillitis, pharyngitis, stomatitis, as well as lymphadenopathy (2). Rarely, infection can also occur in the eye, oculoglandular, which is characterized by conjunctivitis, ulcers, and lymphadenopathy. Septic infections are systemic and do not have localized swelling of lymph nodes – this clinical presentation often occurs in conjunction with other symptoms. Inhalation of the bacteria results in one of the more severe forms of disease, pneumonic tularemia. It has been reported that as few as 10 CFUs of bacteria (6) are capable of causing this type of infection. In this form of disease, the febrile illness symptoms occur, as well as coughing and chest pain. If left untreated, the mortality is approximately 40% of all cases of pneumonic tularemia. All forms of tularemia can cause lasting symptoms for weeks and require an antibiotic regime for 10-21 days (7).

1.1.1.1 Focus on Aerosol Infections

In the Reed Lab, the primary focus is infections of the respiratory tract and aerosol inoculation. Inhalation of *F. tularensis* by small particle aerosol has been shown by the Reed Lab and others to have an extremely low infectious dose and results in a serious disease depending on model organism and bacterial strain (8). In addition to its low infectious dose, *Francisella* species are relatively stable when aerosolized either naturally or manually in the lab setting and are relatively simple to produce in mass quantities. These characteristics of this bacteria as well as its history have led the Center for Disease Control (CDC) to classify it as a Tier 1 Select Agent, which are biological specimens that have the highest capability/likelihood of being weaponized (9). In 1969, the U.S. renounced their offensive biological weapons program, which included research into weaponizing *Francisella* species. In 1972, the U.S. and several other countries signed a treaty at the Biological Warfare Convention agreeing to cease production of biological weapons. However, the U.S.S.R., a signee of the treaty, continued to produce bioweapons, including *Francisella* (10). In addition, *F. tularensis* has caused outbreaks when aerosolized naturally, such as during the periodic “lawnmower tularemia” cases seen in Martha’s Vineyard (11). These cases were caused when rabbit dens were unintentionally run over by lawnmowers during routine maintenance, aerosolizing the bacteria.

1.1.2 Epidemiology of Natural Francisella Infection

Francisella species are endemic almost exclusively to the Northern Hemisphere, as shown in **Figure 1** (12). Subspecies *tularensis*, the most virulent subspecies, is found primarily in the U.S. *Ft. holarctica* is more widespread and is found in Europe and across Asia as well as North America.



Figure 1 Global distribution of all subspecies of *F. tularensis*.

In the U.S., cases are primarily seen in the Midwest and Central states with some outbreaks in other states. **Figure 2** is from the CDC’s database showing tularemia cases reported from 2018 (13). Cases in the U.S. are relatively rare, making this disease difficult to diagnose (7).

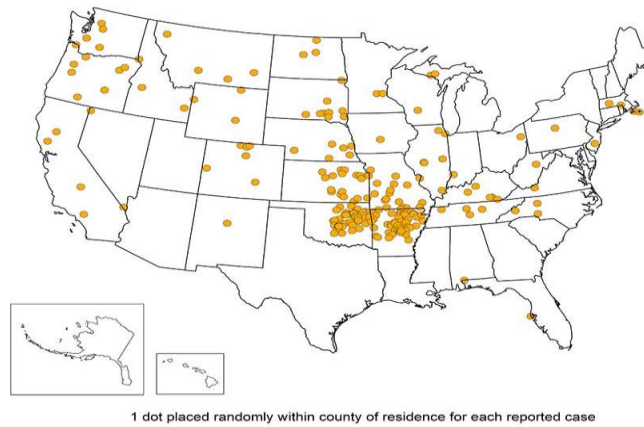


Figure 2 U.S. Cases of Tularema in 2018.

1.2 Immune Response to *Francisella tularensis* and Current Vaccine Strategies

1.2.1 *Francisella tularensis* Pathogenesis and Host Response

Unlike other gram negative bacteria such as *Escherichia coli*, *F. tularensis* lipopolysaccharide capsule does not serve as an endotoxin (14). Instead, it is currently thought that the tissue damage and subsequent disease is caused by a large bacterial burden within the tissues and blood (15) and is partially mediated by the host response. During infection, *F. tularensis* has the ability to infect many different cell types, including erythrocytes (16), splenocytes, hepatocytes, neutrophils, dendritic cells, and macrophages (17). When phagocytes engulf *F. tularensis* bacteria, the immune cells begin to undergo normal development of the phagosome microenvironment until the bacteria escape and enter the cytoplasm of the cell (18). While this mechanism is not fully elucidated, it is thought that *F. tularensis* is able to prevent the acidification of the phagosome and this in turn allows the bacteria to destabilize the membrane of the phagosome (18, 19). Once inside the cytosol of the host cell, *F. tularensis* begins to produce specific proteins required for intracellular growth. Some of these products are known, such as the IglC protein required for escape and intracellular growth; but, most are hypothetical proteins with hypothesized functions (18, 20).

Virulent strains of *Ft. tularensis* are often characterized by a generalized immune suppression during early infection (14, 15, 21, 22), allowing the bacteria to reproduce to high titers in the host and subsequently contribute to virulence. Following this, infection results in a robust immune response involving both IgM (23), IgA and hypercytokinemia (24). A robust immune response is seen earlier and is less severe in avirulent strains, such as LVS and *F. novicida*, which is widely thought to contribute to the fact that these strains do not cause severe disease in humans

(22). Pneumonic tularemia results in respiratory distress and occasionally bacteremia in rabbits and mice (8, 25-27).

1.2.2 Vaccine Strategies

Licensure of a vaccine in the U.S. to protect against *F. tularensis* infection is currently only possible using the FDA Animal Rule. This rule states that, in cases where it would be unethical or immoral to conduct human trials against a pathogen, animal models may be used instead of phase III clinical trials (28). Since outbreaks of *F. tularensis* are rare, it would be difficult to test the efficacy of a vaccine candidate by challenging humans, although it has been done in the past (29, 30). Another stipulation of the FDA Animal Rule is that the exact mechanisms of protection elicited by the vaccine must be characterized. The debated role of antibodies (see **Table 1**) in protection against *F. tularensis* thus warrants further investigation as indicated by the Animal Rule.

Vaccination efforts for *F. tularensis* began in the mid-1900s with killed vaccines produced by Lee Foshay (30) who used acetone or phenol to prepare samples. These efforts resulted in a reduced incidence of disease among lab workers and comparatively more mild disease presentation than those who were unvaccinated. However, killed vaccines have been shown to be largely ineffective due to the lack of cellular immune response (4, 31, 32). Later, groups attempted to use subunit vaccines with the immunogenic antigens from *Francisella's* lipopolysaccharide (LPS) outer membrane or the O-antigen sugars attached to LPS (33).

USSR researchers created an attenuated live vaccine from *Ft. holarctica* (type B) strain, naming it the “Live Vaccine Strain” (LVS). This strain is used in the U.S. as an investigational new drug, but is unlikely to be licensed due to its side-effects and unknown exact method of attenuation (32). Recent studies in the Reed lab have examined other live-vaccine candidates that

are mutants of the virulent Schu S4 strain: $\Delta aroD$, $\Delta guaBA$, and $\Delta fipB$ (34) in the rabbit model. The AroD mutant conferred 83% protection and warrants further investigation in its use as a vaccine. In these experiments, I used rabbit plasma produced from these hyperimmune animals. “Hyperimmune” rabbits are animals that have been exposed to *F. tularensis* a total of three times. Rabbits were exposed to AroD twice in a prime-boost vaccination, then challenged with a high-dose of Schu S4. Surviving animals (83%) were then used as hyperimmune samples (35). Survivors exhibited higher IgG titers and little or no clinical symptoms of infection.

1.3 Humoral Immunity in *F. tularensis* Infections

Antibodies are proteins produced by B cells in the body to fight against many different pathogens, including intracellular bacteria such as *Francisella* species. The fragment antigen binding (Fab) portion of these proteins are highly specific to a certain epitope on the targeted bacteria. Once bound, the fragment crystallizable (Fc) region of the protein binds to different receptors on immune cells that subsequently produce a wide variety of responses (31). These responses may include direct killing or agglutination of the bacteria, induction of complement proteins that kill the bacteria, or uptake of the pathogen into immune cells such as macrophages (31). While these mechanisms are relatively well known across different infections, the exact roles antibodies play in *Francisella tularensis* infections is not.

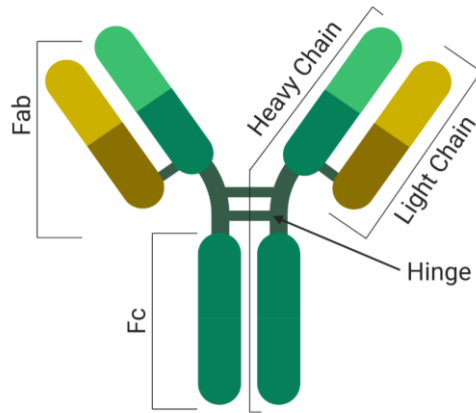


Figure 3. Schematic diagram of IgG.

Table 1 shows a visual summary of different articles that examined the use of *Ft* antibodies in protection. In Stenmark’s and Kirimanjeswara’s work, it was found that antibodies were able to reduce bacterial burden in animal models (36, 37). Upon investigation of mechanisms, Kirimanjeswara found that the process was not complement-mediated but facilitated by FcγR. This finding is important because FcγR are known to mediate phagocytosis, a key event in the life cycle of *F. tularensis*. However, Schwartz’s work (23) indicates that complement is mediated through IgM, and this functions in bacterial killing while other studies indicate that complement receptors facilitate uptake of bacteria but may not result in phagocytes killing *Francisella* (38). This is important to note because the receptors involved in phagocytosis may facilitate the intracellular route of the bacteria, at least initially during infection (38). Other papers (39) conclude that B cells but not antibodies function in protection against bacterial infection. Due to these conflicting conclusions, the role of antibody during infection is not yet well understood and thus requires investigation.

As previously mentioned, elucidating the exact roles of antibodies in vaccination and protection is paramount to vaccine licensure under the FDA Animal Rule. Antibodies produced

by rabbits vaccinated with mutant strains of *Ft. tularensis* and *Ft. holarctica* will bind to multiple antigens, both inside and outside the *Francisella* bacterium (25). In addition, the Reed Lab has also found that IgG titers in rabbits vaccinated with Schu S4 Δ AroD in a prime-boost schedule had a weak correlation with survival from virulent Schu S4 challenge. In immunoproteomic studies of *F. tularensis*, researchers found that multiple exposures to *Francisella* resulted in an increase in antibody titer as well as a broader range of specificity to antigens (40-42). In fact, these studies show that initial exposure to *F. tularensis* resulted in antibodies specific to outer membrane antigens, such as LPS or the O-antigen but subsequent exposures produced antibody responses against cytoplasmic antigens. Antibodies used in this study likely follow this pattern, since the rabbits used to produce the antibodies were exposed to *F. tularensis* multiple times. While many groups have examined effects of plasma or monoclonal antibodies, no one has yet to examine the effects of a pure polyclonal antibody cocktail produced from multiple exposures of *F. tularensis* in rabbits. Since pre-challenge IgG titers loosely correlated with survival (35), we thought that these antibodies might be playing a role in protection and we could replicate experiments produced by other groups using hyperimmune rabbit antibodies.

Table 1. Summary of Literature Examining Passive Protection Against *F. tularensis*.

First Author	Year	Mouse Model(s) Used	Strain (vaccinated to produce Ab)	Strain (challenged)	Abs used	Exposure	Results
Kirimanjeswara, G. S. (36)	2007	multiple mouse strains	10 ³ CFU LVS (i.n)	10 ⁴ CFU LVS (i.n)	250 ul (i.p) (mouse sera)	pre/post	survival (pre), prolonged illness (post)
Savitt, A. G. (43)	2009	BALB/c, CH3HeN	10 ⁵ CFU LVS (i.d)	7 x 10 ⁷ LVS	50 ug in 200 ul (in-house Mabs)	pre/post	survival (pre), prolonged illness (post)
				24 CFU SCHUS4		pre-exposure	prolonged illness
Steiner, D. J. (44)	2018	BALB/c	< 10 ² CFU LVS (prime), 10 ³ LVS (boost) (i.n.)	24-31 cfu SCHUS4 (i.n.)	250 ul (i.p) (mouse sera)	pre-exposure	survival when AMs depleted only
Drabick, J.J. (45)	1994	C3H/HeN	LVS in humans	10 ⁴ LVS (i.p)	200 ul (i.p) (human sera)	pre-exposure	survival
Stenmark, S. (37)	2003	C57BL/10, C57BL/10- <i>Igh-6^{m1Cg}</i>	5 x 10 ³ CFU LVS in C57BL/10	6 x 10 ⁷ CFU LVS (i.d.)	.5 ml (i.p.) (mouse sera)	pre-exposure	survival
				1st: 5 x 10 ⁴ CFU LVS (i.d.)		pre-exposure	survival
				2nd: 3 x 10 ⁸ CFU LVS (i.d.) (5wk later)		pre-exposure	survival
Fulop, M. (46)	2001	BALB/c	50 ug LPS (x3) (i.p.)	7.1 x 10 ⁴ CFU LVS	.4 ml (i.p.) (mouse sera)	pre-exposure	survival
			above + 10 ⁶ CFU LVS (i.p.)	100 CFU SchuS4	.4 ml (i.p.) (mouse sera)	pre-exposure	no significant difference
Francis, E. and Felton, L.D. (47)	1942	white mice	Ft in horses, sheep, rabbits or humans	Japanese strain (LVS)	1 cc (i.p.) (various animals)	at same time or right after challenge	prolonged illness
Pannel, L. and Cordle, M. (48)	1962	Swiss-webster mice	1ml sublethal dose of Jap strain <i>P. tularensis</i>	.5 ml lethal dose of Jap strain P.t. (i.p.)	.5 ml (i.p.) (mouse sera)	mix w/ challenge	survival
			1 ml filtrate from 10 ³ cells/ml of Jap strain P. tul	.5 ml lethal dose of Jap strain P.t. (i.p.)	.5 ml (i.p.) (mouse sera)	mix w/ challenge	prolonged illness
Allen, W.P. (49)	1962	Swiss mice, A/LN mice	killed whole cell SchuS5 (10 x 10 ⁷ cells/ml) .5ml for 5 days	SchuS5	.25 ml (i.p) (mouse sera)	pre-exposure	prolonged illness
Chou, A.Y. (39)	2017	C57BL/6J and C57-BKO	10 ¹ CFU U112 (i.d.)	10 ⁵ or 10 ⁶ CFU U112 i.p.	.5 ml serum + 10 ¹ CFU U112 i.d.	pre-exposure	no significant difference

1.3.1 Passive Immunization and Therapeutics

Initial studies of *F. tularensis* focuses heavily on passive immunization and protection using plasma from vaccinated subjects (29, 47, 48). Many studies found that plasma injected directly into animals protected against infection from LVS but often failed to confer protection against virulent Schu S4 challenge (see **Table 1**). **Table 1** only shows immunization studies performed in mice since passive immunization experiments in this work were performed in mice. However, there is one study in the Fisher rat model that showed successful passive immunization against Schu S4 challenge (50). More discussion regarding the use of different models can be found in section 1.4.2. In studies examining post-exposure inoculation with plasma, researchers found that immune plasma injections enabled mice to survive longer than controls against lethal LVS infection (36, 43). While these results may not have shown full protection, the data do support the notion that antibodies could potentially be used as a supportive therapy following an exposure to *F. tularensis*.

The passive immunization experiments performed in this study used two different animal models in experimental design: antibodies derived from outbred New Zealand White (NZW) rabbits were given to BALB/c mice. More details regarding differences in animal models can be found in section 1.4.2, but in brief this method has not yet been performed to examine antibodies against *F. tularensis*.

1.4 Working with *Francisella tularensis* in the Laboratory Setting

1.4.1 Biosafety

The more virulent strains of *Francisella tularensis* are classified as BSL3 pathogens, meaning that laboratory work on these agents must be performed in stringent BSL3 labs. Of the strains mentioned in this study, *Ft tularensis* (type A) SCHU S4 and SCHU S4 Δ aroD are both classified as BSL3 pathogens. Other strains, such as *Ft. holarctica* ATCC LVS and RML LVS are BSL2 pathogens. In studies involving animals infected with the more virulent strains, work must be performed in high-containment laboratories. This means that lab workers must wear both waterproof gowns or suits and gloves as well as respiratory protection. In addition, workers must follow special protocols upon bringing out samples from inside the BSL3 facility into the BSL2 workspace to ensure any viable pathogen is inactivated. Work in high containment labs traditionally evolves more slowly than other labs due to these constraints.

1.4.2 Animal Models for *Francisella* Infections

Development of different animal models to examine infection of *F. tularensis* is an additional requirement that researchers face in accordance with the FDA Animal Rule. Each animal model has benefits and downfalls in vaccine development. The Reed lab has worked extensively on showing that the rabbit model of infection with *F. tularensis* recapitulates what is seen in humans (8, 25, 34, 35, 51). Most notably, rabbits do not develop a severe illness when exposed to LVS, like humans. This is a major benefit of the rabbit model over the mouse model since the virulence between LVS and other type B strains and especially type A strains has been

shown to be dramatically different. Specifically, mice succumb to infection with LVS while other models (rat, monkey, rabbit, human) do not. This allows research using the rabbit as a model to translate into human disease and treatments. Rabbits are not common models of infectious diseases, creating challenges in logistics and reagent supplies available. For example, it is common to have commercially available antibodies produced in rabbits but can be difficult to find commercial antibodies against rabbits. Mice are suitable models for disease in preliminary studies since they are relatively cheap and work with LVS can be done under BSL2 conditions. This makes mice an attractive model for many researchers, resulting in numerous papers using murine models. As mentioned earlier, this model for disease may not translate to human disease, directly conflicting with the FDA Animal Rule requirements needed to generate a vaccine.

Other animals have also been used to model tularemia. The non-human primate (NHP) model of disease shows similar clinical presentation of infection with different strains of *F. tularensis* as the rabbit model (8, 52). However, NHPs are expensive to obtain and maintain, making this an unlikely animal to be used in preliminary studies. Recent research using the rat as a model has been promising in relating to the human model more so than the mouse (53). However, this animal appears to be resistant to lethal infection of Schu S4 in comparison to the NHP model, as indicated by the difference in lethal doses (52, 53).

1.5 Public Health Significance

Due to its high infectious capability, ease of aerosolization, and ease of mass production (54), *Francisella tularensis* has been deemed a Tier 1 Select Agent by the CDC and the USDA as part of the Federal Select Agent Program. This means that *F. tularensis* has a high likelihood of

being used as biological weapon compared to other pathogens in the Select Agent Program. Thus, while naturally-occurring infections have been dramatically lowered in the U.S. since the 1940s to about 200 cases/year (55), there is still a prerogative to develop protective measures against this disease. Currently, the Live Vaccine Strain (LVS) is the only vaccine available; however, it has not been approved by the FDA for regular use. There are other strains of attenuated *Francisella* that are used as candidate vaccinations, some of which have been studied in the Reed Lab (34, 35). Diagnostic tests for infection include PCR of blood samples, cultures and antibody titers (56). Treatment by several antibiotics such as streptomycin, gentamycin, and fluoroquinolones are available and effective (7).

2.0 Specific Aims

The aim of this study was to examine the effects that antibodies have on the intracellular bacteria *F. tularensis*. Many studies claim that immunity to *F. tularensis* is largely cellular and the exact roles of antibodies during infection is not well defined. In previous studies, plasma injected into mice prior to challenge has been shown to prevent disease from LVS but results vary when animals were challenged with virulent strains. Since the rabbit model produces a more diverse antibody repertoire after prime-boost vaccination than is seen in mice, we wanted to determine if these antibodies were more effective at controlling infection than previously shown. This would show that, contrary to popular belief, antibodies do play a role in the protection against *Francisella* infection.

2.1 Aim 1: Purify and Characterize Antibodies Produced from Hyperimmune Rabbit

Plasma

- (a) Determine the optimal concentration of ammonium sulfate required to precipitate out all antibodies from rabbit plasma.
- (b) Examine the antibodies purified from hyperimmune rabbit plasma by purification, binding, and concentration.

Hypothesis:

1. The use of caprylic acid in addition to ammonium sulfate will precipitate out antibodies from rabbit plasma that are relatively pure, highly concentrated, and have strong avidity to *Francisella*.

2.2 Aim 2: Examine the Potential Role of Antibodies in Protection Elicited by Vaccination

- (c) Examine the effects of antibodies binding to RML LVS using bacterial titers and traditional agglutination and complement fixation tests.
- (d) Infect J774A.1 macrophage-like cells with *Francisella* coated in antibody to examine increases in phagocytosis and intracellular growth.
- (e) Passively immunize BALB/c mice and challenge using aerosolized RML LVS to determine if antibodies can protect against death.

Hypotheses:

1. Antibodies produced by hyperimmune rabbits bind to RML LVS bacteria, causing an increase in phagocytosis in J774A.1 cells.
2. These antibodies, when administered prior to infection, can protect BALB/c mice against lethal aerosol infection of RML LVS.

3.0 Materials and Methods

3.1 Animal Models Used and Biosafety

All animals used during the experiments were housed in pathogen free isolation caging inside the Regional Biocontainment Laboratory (BSL3+). Six-to-ten-week-old female BALB/c mice were obtained from Charles River and used in experiments where indicated. Mice were allowed to adjust to the new cages for 48 hours before any additional handling. All work using Select Agents, such as the SchuS4 isolate of *F. tularensis*, were manipulated in a BSL 3+ lab.

3.2 Antibody Purification

Immune and naïve rabbit plasma were purified through a two-step process using caprylic acid and precipitation through ammonium sulfate. In the first step, 10 ml of plasma from either immune or naïve rabbits was thawed and spun at 10,000x g at 4°C for 30 minutes. The supernatant was filtered through Millex .8 µm filters, then twice the volume of .6M sodium acetate buffer was added to the supernatant. For a volume of 10ml of filtered plasma, 820 µl of caprylic acid was added, dropwise, while stirring, at room temperature (57). After allowing the solution to stir for another 30 minutes at room temp, it was then spun at 4,000x g for 30 min at 4°C and dialyzed in PBS overnight with 2-3 buffer changes.

In the second step, immunoglobulin was precipitated out of the solution using saturated ammonium sulfate. Ammonium sulfate was added dropwise to the dialyzed supernatant at 4°C,

while stirring, until a final concentration of 43% was reached (58). This solution was spun at 10,000x g for 30 min at 4°C. The pellet was resuspended in 2ml of PBS for future analysis. In addition, all fractions from previous steps were saved for analysis (ie. caprylic acid precipitate, plasma pellet, etc.).

3.2.1 Optimization of Purification of Antibody

The method described above was initially optimized using gradually increasing amounts of ammonium sulfate. In the initial purification procedures, ammonium sulfate was added dropwise until a concentration of 23% was achieved. The solution was spun at 10,000x g at 4°C for 30 minutes. The supernatant was removed for further purification and the pellet, if any, was resuspended in PBS for further analysis. Ammonium sulfate was added to the supernatant at 4°C dropwise, while spinning, until a final concentration of 33% was achieved. The solution was spun down and separated as before. This process was repeated to achieve a concentration of 43% ammonium sulfate. Each product was collected for future analysis to determine which contained the largest amount of antibody. Analysis of antibody purity and concentration was performed through SDS gels and BCA assays. Binding was assessed through ELISA analysis.

3.3 SDS Gel Analysis

Proteins fractions from each step in the purification process were used for SDS-PAGE gel analysis [adapted from (59)]. For each lane, 15 µl of protein sample was mixed with 5µl of Laemmli 4x sample buffer. Each sample was boiled at 95°C for 5 min, then placed on ice for at

least 5 min before loading into gel. Bio-Rad Mini-PROTEAN® TGX™ Precast Gels (4-20%) were used in conjunction with the Bio-Rad PowerPac™ Basic Power Supply as well as the Precision Plus Protein™ Kaleidoscope™ Prestained Protein Standards as the ladder. Before using, the comb and metal strip of the gel was removed, placed in the chamber, and filled to the 2 gel (approximately 1L) line with Bio-Rad 1x loading buffer. Each lane was loaded with 7µl of sample mix or ladder and allowed to run at 100 V for approximately 60 min. Once the samples had run, the gel was removed and stained using Coomassie Blue and Coomassie Blue de-stain (60).

3.4 Enzyme-linked Immunosorbent Assay (ELISA) Analysis

Enzyme-linked immunosorbent assays were developed in-house by other members of the Reed lab (Le’Kneitah Smith, Elizabeth Stinson, Katherine O’Malley Willett, manuscript in preparation). Hyper-immune rabbit plasma was used as a positive control, as established in-house, and commercial rabbit low-binding IgG was used as a negative control. In general, high-binding 96-well plates were coated with heat-killed SchuS4 and allowed to sit overnight at room temperature. Coating antigen was removed and replaced with blocking buffer, which was allowed to incubate at 37°C for 3 hours. Once the incubation period was over, plates were washed 5 times with 0.005% Tween in PBS and stored at 4°C or used immediately for assay.

Samples were diluted as indicated in PBS-T (1:50 for positive and negative controls), which was subsequently diluted by half-logs in duplicate on the plate, with the last row void of sample. The plates were then incubated at 37°C for 1 hour, after which they were washed 5 times with PBS-T. Once washed, plates were coated with secondary HRP-conjugated antibodies (either anti-IgG or anti-IgM), incubated at 37°C for 1 hour and washed again 5 times with PBS-T. After

washing, POD Chemiluminescence working solution was added and allowed to sit at room temp for 3 min before absorbance was read at 405nm. Analysis was done in the Prism software.

3.5 Bicinchoninic Acid (BCA) Assays

Protein concentrations were determined using the Peirce BCA Assay kit and respective protocol(61). Briefly, a standard curve was established using known concentrations of BSA in PBS. For each standard and sample, 1 part sample/standard was mixed with 20 parts working reagent (1:50 of BCA Reagent B and A, respectively) and allowed to incubate at 37°C for 30 min. Measurement of protein concentration was performed through spectrophotometric analysis at 562 nm. Concentrations of samples were determined through Prism software interpolation using the standard curve of BSA. Since the assay only determine protein concentrations between 20 and 2,000 µg/ml, the samples were diluted to 10% or 2% in PBS.

3.6 Cell Culture

J774 cells were maintained by serial passage in DMEM supplemented with l-glutamine, 10% FBS, 1% penicillin-streptomycin, and 1% HEPES buffer. When required for infection, cells were washed 3 times with PBS and scraped from tissue culture flasks. The cells were seeded into a 12-well plate treated for culture and allowed to incubate for 24 hours before use.

3.7 Bacterial Methods and Culture

Francisella tularensis strain RML (Rocky Mountain Labs) LVS was obtained from Catherine Bosio and streaked onto CHA for isolation using a sterile loop. Two days later, individual colonies were selected using aseptic technique and used to create a bacterial slurry in PBS that was approximately 0.06-0.08 optical density (OD) at a wavelength of 600nm. Five-hundred microliters of this slurry was added to 29.5 ml of brain heart infusion (BHI) supplemented with cysteine and ferric pyrophosphate. The culture was incubated for 16-18 hours at 37°C in a shaking incubator set to 200 RPMs. After the culture was allowed to grow, it was harvested with a desired OD of approximately 0.1-0.3.

3.7.1 Determining Aerosol Dose of RML LVS

Aerosol doses were determined as previously performed by the Reed Lab (62). In general, bacteria slurries were aerosolized using a Collison 3-jet nebulizer for 10 minutes. The nebulizer was controlled by the AeroMP exposure management system (Biaera Technologies, Hagerstown, MD). The AeroMP monitored and controlled all environmental parameters in the exposure chamber (relative humidity, temperature, pressure, air input and exhaust). Aerosol sampling was done using an all-glass impinger (AGI-4). The nebulizer was operated at 7.5 lpm, 25-30 psig while the sampler was operated at 6 lpm, 7-12 psig. For rodent exposures, a whole-body exposure chamber (39 l total volume) was used which can hold four metal exposure cages at a time with up to 10 mice per exposure cage. Chamber airflow rates were set to 19.5 lpm for both input and exhaust, to insure 0.5 air changes/minute in the chamber. For *F. tularensis*, a humidification loop was also added to input air to insure relative humidity is at least 65%, based on prior studies in the

Reed lab indicating that humidification must be high for good aerosol performance (62). The Collison 3-jet nebulizer creates a small-particle aerosol (1-2 μm mass median aerodynamic diameter) of bacteria in liquid media that flows at an even rate through the rodent whole-body chamber. This allows the animals to move freely inside the mesh cages within the chamber while being exposed from both the top and bottom of the chamber in order to maximize efficiency. Aerosol doses are calculated after determining the aerosol concentration of the pathogen from the AGI sample. Results from previous rodent exposures using the same experimental conditions were used to calculate the starting bacteria concentration needed to achieve desired target doses. Inhaled or presented dose is calculated as the product of the aerosol concentration, the duration of the exposure (10 minutes) and the minute volume of the animal. For mice, Guyton's formula is typically used to calculate minute volume rather than empirical determination; Guyton's formula stipulates that minute volume is a function of the weight of the animal (63). The following formulas summarize the calculation of the inhaled dose:

$$\textit{Inhaled dose} = [\textit{Aerosol}] \times \textit{exposure time} \times \textit{minute volume}$$

$$[\textit{Aerosol}] = \frac{[\textit{AGI}] \times \textit{AGI volume}}{\textit{AGI flow rate} \times \textit{exposure time}}$$

3.8 LVS Infection of J774 Macrophages

Infections of J774 cells were performed in BSL2 using sterile techniques. Two days prior to infection, LVS (either ATCC strain or RML strain) were streaked onto CHA for isolation. Cells were counted with a hemocytometer and seeded at 3×10^5 cells/ml in 12-well plates 24 hours prior to infection. On the day of infection, single colonies were selected and vortexed in PBS in order to achieve a bacterial slurry with an OD of 0.1-0.3 at 600nm – the linear range of growth for *F. tularensis*. The concentration of bacteria in the slurry was determined using a previously established standard equation for *F. tularensis* (62). This was then diluted with the appropriate amount of PBS in order to achieve a multiplicity of infection (MOI) of 100:1 of LVS to J774s. Once diluted, 100 μ l of this slurry or PBS as a control was added to each well in the 12-well plate. After the bacteria infected the cells for 2 hours, 2 ml of PBS with 50 μ g/ml of gentamycin was used to wash each well 3 times. After washing, 1 ml of DMEM supplemented with 50 μ g/ml gentamycin, 10% FBS, and 1% HEPES buffer was added and incubated for another 45 minutes to 1 hour.

Following the second incubation, the media in wells for timepoints 24hrs, 48hrs, and 72hrs were removed and replaced with DMEM supplemented with 2 μ g/ml gentamycin, 10%FBS, and 1% HEPES. The media in the 0hr timepoint wells were removed and washed 3 times with 2 ml of PBS. J774 cells were lysed by incubating 1ml of 0.02% SDS in dH₂O at room temp for approximately 10 minutes as well as mixing with a pipette 10 times. This solution was serially diluted in PBS to 10⁻⁶. Each dilution was plated in triplicate using the drop method, and 200 μ l of the undiluted solution was plated in duplicate on CHA plates and spread using an L-shaped spreader. Bacteria were quantified 3-4 days later by counting colony-forming units on plates.

3.9 Opsonization of LVS

Opsonization was assessed as enhanced uptake of *F. tularensis* by J774 cells after incubating bacteria with specific antibody. RML LVS was suspended in PBS to create an initial slurry, then diluted down to accomplish a concentration of 3×10^8 CFU/ml as described above. This slurry was then incubated with 10% of the antibody solution (500 μ g/ml in PBS) at 37°C for 30 minutes. Antibodies purified from naïve rabbits were used as a control as well as PBS with no antibodies added. After incubation, the slurries that were used to infect J774s in opsonization infection assays were used directly as the inoculum in the assay described in the previous section. Slurries were serially diluted out to 10^{-8} and plated onto CHA using the drop method. Colonies were enumerated approximately 3 days later concentration (CFU/ml) was calculated.

3.10 Complement Fixation of RML LVS

Complement fixation assays were performed based on an established protocol (64). Slurries of RML LVS were prepared using culturing methods mentioned in section 3.7. Approximately 3×10^8 CFU/ml of RML LVS were combined with 10% antibody solutions of varying concentrations and 10% rabbit complement (MP Biomedicals™). Antibody solutions from both hyperimmune and naïve rabbits were diluted to 1:10, 1:100, and 1:1,000 of the original 500 μ g/ml solution. The naïve rabbit antibody, PBS with complement, and PBS without complement were used as negative controls. All slurries of RML LVS with antibody/complement or PBS solutions were incubated at 37°C with 5% CO₂ for 30 minutes. Bacterial titers were enumerated

by serially diluting each slurry and inoculating the dilutions onto CHA plates. The CFUs produced were counted 2 days later.

3.11 Agglutination Tests of RML LVS

Agglutination tests have historically been used to determine immune response in tularemia patients. The agglutination tests in these experiments were based on an established protocol for microagglutination testing for tularemia in humans (65, 66). The antigen was prepared by creating a slurry of RML LVS that was approximately 1×10^9 CFU/ml. Formalin and Safranin were added to the solution for a final concentration of 0.5% and 0.005%, respectively. The antigen stock was later serially diluted by 2 until a dilution of 1:128 was achieved, then kept in 4° C until the assay was performed. Hyperimmune antibody solution was serially diluted by 2 in PBS in a U-bottom, 96-well plate starting at 1:10 and stopping at 1:10,240 dilutions. The last column of PBS alone served as the negative control. Antigen dilutions were then added to the plate in a 1:1 ratio with the antibody solutions (see **Figure 28**). The plate was incubated at 37°C in 5% CO₂ for 24 hours before being read initially, but was shortened to 4 hours after the first trial. The optimal antigen dilution was determined by the highest dilution of antigen on the plate that produced both positive (no button) and negative (button) agglutination results. The final titer was determined as the highest antibody dilution that produced agglutination in the optimal antigen row.

3.12 LD50 Determination of RML LVS in Aerosol Infection of BALB/c Mice

Three groups of 6-10-week-old BALB/c mice (n = 5) were exposed via the aerosol route to doses of 80, 349, and 1,261 CFUs of RML LVS, respectively. Mice were weighed 24 hours before aerosol infection, and weight was measured once per day until mice succumbed to infection or recovered. Appearance of mice was also measured using clinical scoring, where 1 = normal, 2 = reduced grooming, 3 = oily appearance, 4 = hunched, respiratory distress (euthanasia criteria). Behavior was measured using clinical score scales as well, with 1 = normal, 2 = subdued, 3 = movement when provoked, and 4 = no movement when provoked (euthanasia criteria). Weight loss of 5% or less was designated a 1, 2 = up to 10% weight loss, 3 = up to 15% weight loss, and 4 = up to 20% weight loss. Any animals who lost over 20% of body weight, scored a '4' in either behavior or appearance, or had a cumulative score of '10' were promptly euthanized via intoxication with carbon dioxide, in accordance with AVMA guidelines.

Mice were monitored at least twice per day until a total clinical score of 6 was reached, at which point animals were examined 3 times per day. Animals were monitored daily until complete recovery (total clinical score of 3) or death. After 21 days, the experiment ended, and any remaining animals were counted as survivors and euthanized to collect samples for analysis of bacterial load and serology.

3.13 Antibody Passive Immunization and Subsequent Challenge with Aerosolized RML

LVS

Prior to infection, mice were bled from the submandibular vein and blood from each cage (n = 5, same group) was pooled together for extraction of plasma using the Microtainer plasma separation tubes. Mice were also either ear punched or implanted with IPTT-300 transponders (BioMedic Data Systems) for identification. Approximately 24 hours prior to exposure, animals were inoculated with 500 µg/ml of purified immunoglobulin suspended in PBS from either hyperimmune rabbits or naïve rabbits; PBS alone was also used as a control. In the low-dose exposure experiment, mice were given antibodies via intraperitoneal route (200 µl) or intranasal (20 µl). In the high-dose challenge, mice were injected only through the i.p. route. On the day of infection, 10 mice of the same group were placed into metal cages and exposed to RML LVS through aerosol, using a whole-body rodent chamber. A total of 30 mice were challenged per 10-minute exposure. After infection, animals were observed twice per day. The scoring system and euthanasia criteria were the same as described in the previous section.

After 21 days of infection, all recovered animals were sacrificed and the lungs, liver, and spleens of each were harvested as well as blood. Blood was centrifuged at *10,000x g* for 2 minutes

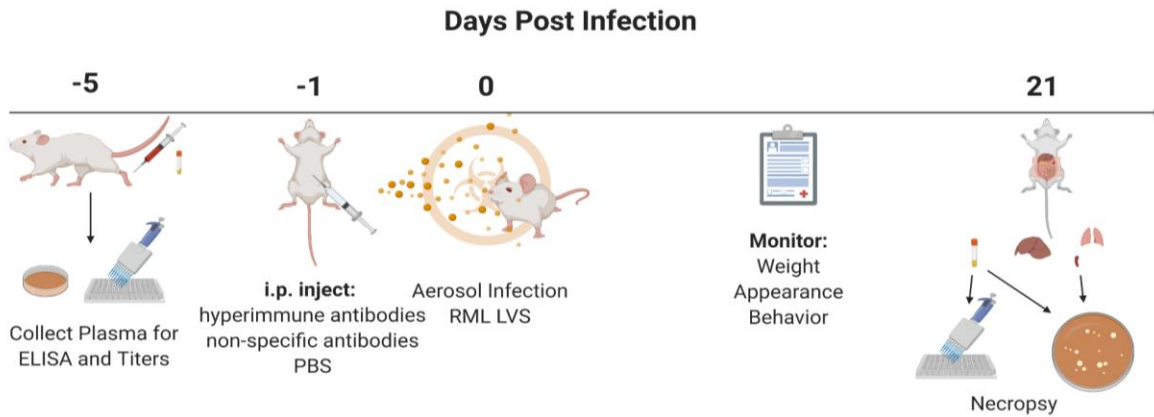


Figure 4. Timeline schematic of BALB/c experiment.

to separate plasma, which was inactivated for future analysis. The remaining clot in the tube was smeared onto CHA plates for qualitative analysis. Harvested organs were frozen over dry ice during necropsy before being transferred to a -80°C . Later, the lungs, liver, and spleens were each weighed, suspended in 1 ml of PBS, and homogenized. This mixture was plated onto CHA using an L-shaped spreader (no dilution) or drop method (10^{-1} to 10^{-6} serial dilutions). Three days later, all colonies were counted in order to determine bacterial burden in each tissue or plasma. If the plates had no *Francisella* growth, samples were incubated an additional 4 days for a total of 7 days.

4.0 Results

4.1 Characterization of Immune Plasma from NZW Rabbit Survivors of SCHU S4 Δ aroD

Prime/Boost Vaccination and SchuS4 Challenge

4.1.1 SDS Gel Purification

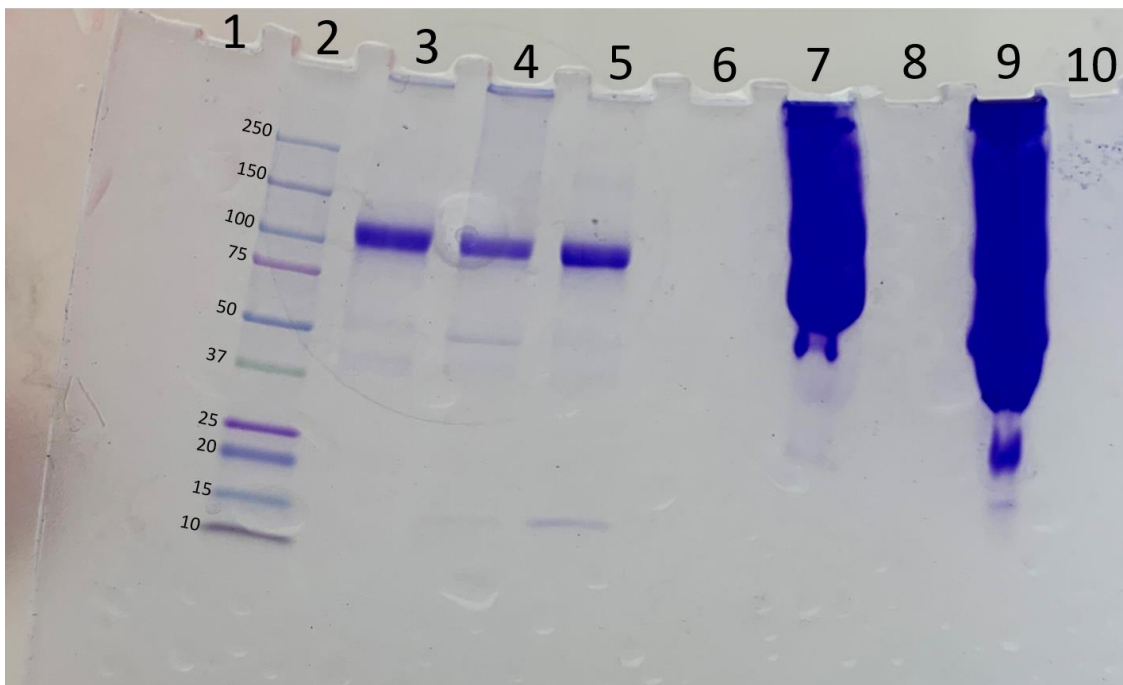


Figure 5. SDS gel analysis of immune plasma purification.

2) Ladder, 3) commercial IgG, 4) 33% ammonium sulfate precipitate, 5) 43% ammonium sulfate precipitate, 6) 43% ammonium sulfate supernatant, 7) caprylic acid precipitate, 9) unfiltered, unpurified hyperimmune plasma. Lanes 1, 8, and 10 are blank but have not been omitted in order to retain integrity of the gel.

A small portion of each sample produced during the protein purification process was saved in order to analyze purity. Figure 5 shows that both the 33% and 43% ammonium sulfate concentrations resulted in a large band that was the same size as that seen in the commercially

purified rabbit IgG. In contrast, there was no detectable antibody in the supernatant of the 43% ammonium sulfate solution. The smaller bands in the 33% and 43% ammonium sulfate pellets likely are either impurities or breakdown products but represent a minor portion of the total protein. Notably, they are also seen in the commercially prepared IgG except for the lower band at approximately 15 kd.

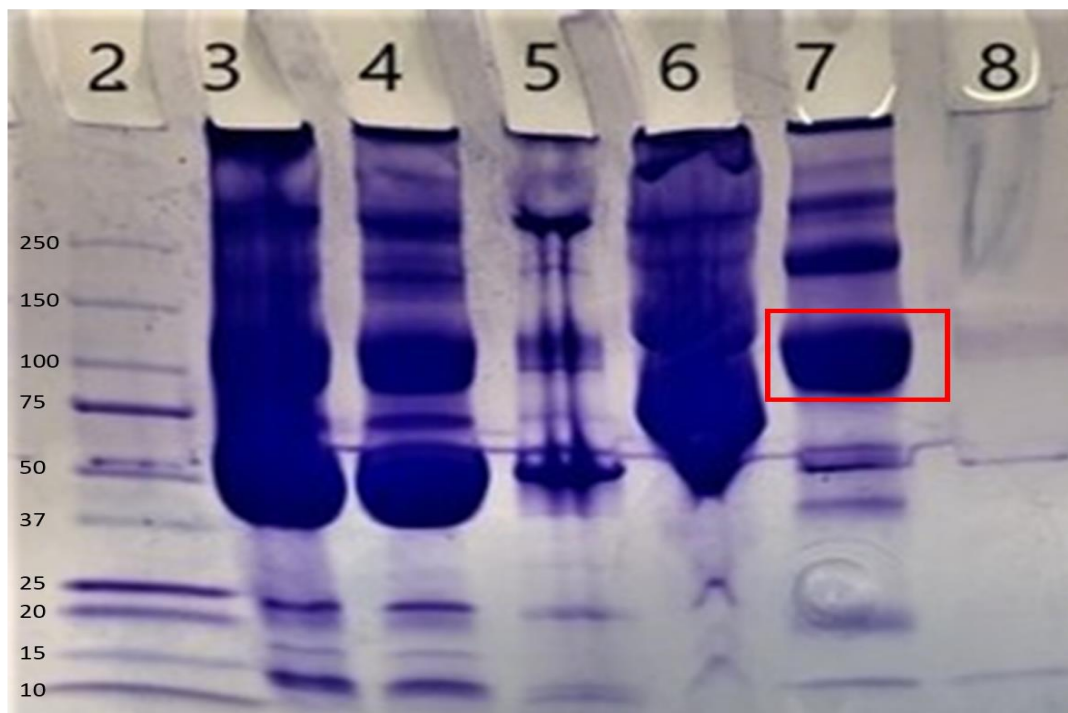


Figure 6. SDS gel to assess purity during each step of the immunoglobulin purification process.

Lanes were as follows: 2) Ladder, 3) unfiltered plasma, 4) filtered plasma, 5) plasma precipitate, 6) caprylic acid precipitate, 7) Immunoglobulin precipitate (43% ammonium sulfate) and 8) 43% ammonium sulfate supernatant. Lanes 1, 9, and 10 were blank (not shown). The red box indicates the band of immunoglobulin purified from the plasma

Figure 6 shows the SDS gel of samples taken of each product during the optimized purification process. Higher concentrations of protein were loaded into this gel than the previous gel in **Figure 5** in order to better assess the purity of the material at each step in the process. While this figure indicates that immunoglobulin is not the only protein in the solution, it does show that the band of antibody is highly concentrated. In addition, the purified product has less background

protein than the unfiltered plasma, which is seen as a large smear down lane 2. This figure shows as a proof-of-concept that the purification process does reduce but does not completely eliminate contaminants in the sample.

4.1.2 ELISA Analysis

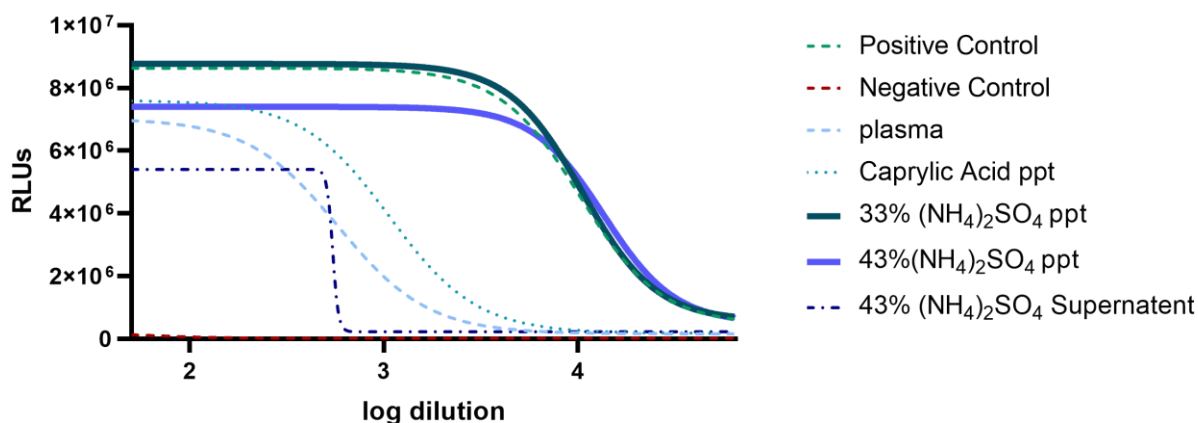


Figure 7. ELISA of immune plasma purification products.

Figure 7 shows a logistic regression analysis of ELISA results for IgG from the various fractions analyzed. EC50 and slope values for each sample produced during the purification of hyperimmune rabbit plasma are shown in **Table 10**. The EC50 value for the 33% and 43% ammonium sulfate precipitate products are relatively the same while the max RLU values are slightly different, as noted by the bolded lines and in **Table 10**. In comparison, the EC50 value of the pre-purification plasma is ~20-fold less than either purification products. Thus, both the 33% and 43% ammonium sulfate solution purified and concentrated *Francisella* specific antibodies. In this figure, all products are normalized to 500 $\mu\text{g/ml}$ concentration while the positive and negative controls remain at their original concentrations. From these results, I determined that the optimal purification process was to spin and filter plasma, then add caprylic acid and spin to remove the

pellet (**Figure 28**), and finally to precipitate out the antibodies (denoted IgG pellet later) using 43% ammonium sulfate solution.

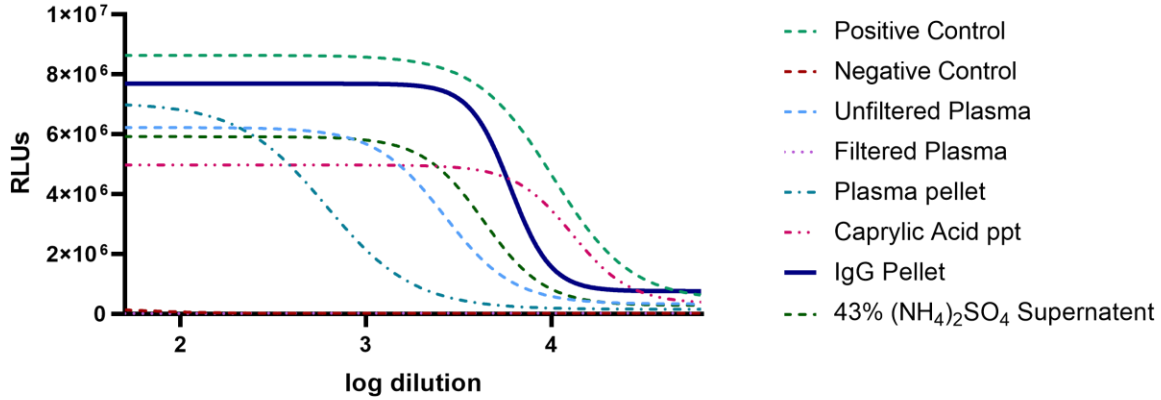


Figure 8. ELISA of Products from Hyperimmune Rabbit Plasma Purification.

Figure 8 shows products from a subsequent purification of hyperimmune rabbit plasma, using the optimized process described above. The EC50 and maximum RLU values are shown in **Table 11**. In this process, the plasma was first spun down at $10,000x$ g before being vacuum filtered. This resulted in less loss of product and no clogging of the filter. The bolded dark purple line represents the antibody pellet produced, which has an overall higher binding as defined by the higher RLU value and higher EC50 dilution than unfiltered plasma from the purification process. The purification product from this process was used in future antibody experiments.

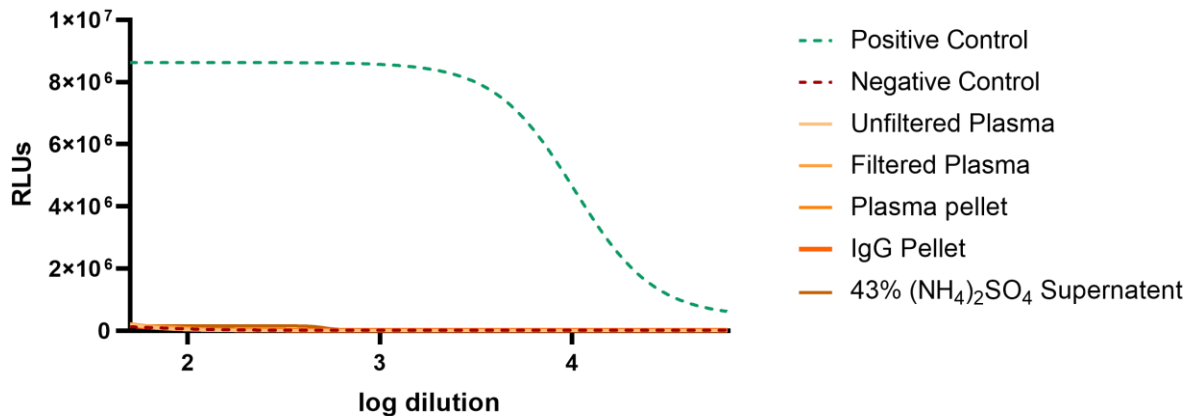


Figure 9. ELISA of products from naive rabbit plasma.

Figure 9 demonstrates a proof of concept of the final, optimized purification process of plasma from a non-immune rabbit. Antibodies purified from this animal's plasma were not *Francisella* specific, which was expected considering this animal was never immunized or exposed to *Francisella*. The only line shown in this graph is the positive control; the other lines all show negative results. The antibodies purified from this rabbit were subsequently used in future experiments as a negative control. In future results, they are denoted as non-specific or non-immune antibodies.

4.1.3 BCA Assays

Table 2. Protein Concentrations from Optimizing Plasma Purification.

Sample	Interpolated Protein Concentration (ug/ml)	Absorbance at 526 nm (10% sample conc.)
Plasma-control		0.98
Caprylic acid purified	13753.74821	0.39
33%(NH ₄) ₂ SO ₄ precipitate	2363.080962	0.16
43%(NH ₄) ₂ SO ₄ precipitate	2247.209513	0.16
43%(NH ₄) ₂ SO ₄ supernatant (undiluted)	4.56519784	Too low

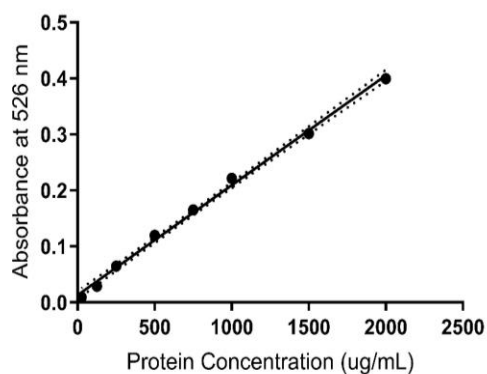


Figure 10. BCA Standard Curve for Optimization Products.

Table 2 shows the protein concentrations for the samples taken during the optimization of the purification process. Interpolated values were calculated using GraphPad software, then multiplied by the dilution factor of the samples. The absorbances are recorded from diluted samples, except the supernatant, which remained undiluted. The standard curve used to determine concentrations is shown in **Figure 10**.

Table 3. Protein Concentrations from Hyperimmune Rabbit Plasma Purification.

Sample	Interpolated Protein Concentration (ug/ml)	Absorbance at 526 nm (2% sample conc.)
unfiltered plasma	70241.78	0.4228
filtered plasma	66652.65	0.4027
plasma pellet	12169.93	0.0995
caprylic acid ppt	5007.782	0.0549
IgG purified	39877.32	0.2530
43%(NH ₄) ₂ SO ₄ supernatant (undiluted)	Too low	0.0146

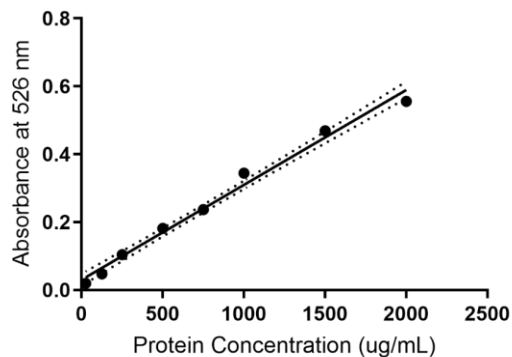


Figure 11. BCA Standard Curve for Hyperimmune Purification Products.

Table 3 shows concentrations of total protein content from each sample during the purification of hyperimmune rabbit plasma. These data were used to generate the 500 µg/ml stocks of antibody used in future experiments. The standard curve used to interpolate the concentrations is shown in **Figure 11**.

Table 4. Protein Concentrations from Naive Rabbit Plasma.

Sample	Interpolated Protein Concentration (ug/ml)	Absorbance at 526 nm (2% sample conc.)
unfiltered plasma	84260.68571	0.363233333
filtered plasma	74026.91871	0.3267
plasma pellet	17665.49514	0.132933333
IgG purified	43624.41384	0.218166667
43%(NH4)2SO4 supernatant (undiluted)	534.1016746	0.157766667

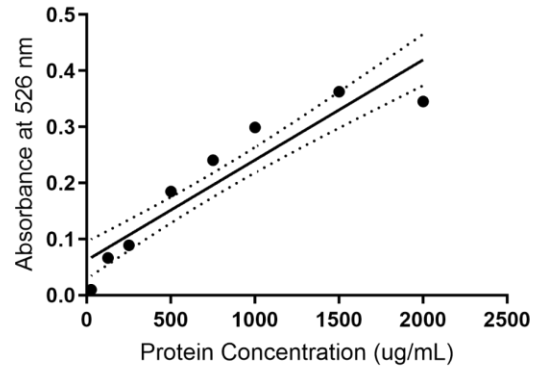


Figure 12. BCA Standard Curve for Naïve Rabbit Plasma Purification.

Table 4 shows the concentrations of protein content from samples during the purification of the naïve rabbit plasma. The interpolated concentration for the purified antibody was used to generate the 500 µg/ml stock used as a negative control in future experiments. The standard curve used to generate the interpolated concentrations is shown in **Figure 12**.

4.2 Effects of Antibodies on RML LVS

4.2.1 Opsonization

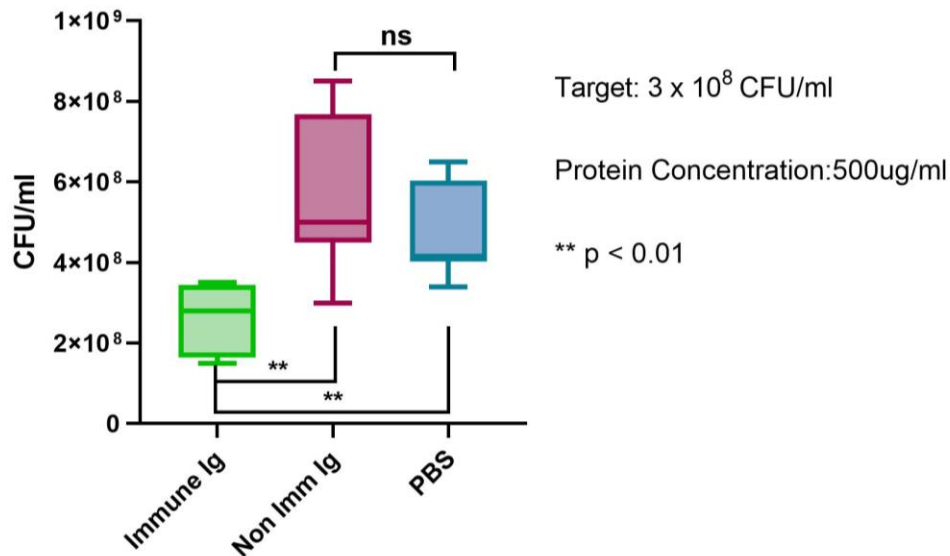


Figure 13. Incubation of immune antibodies and *F. tularensis* RML LVS result in lower bacterial titers.

Figure 13 is a compilation of multiple experiments ($n = 8$) examining the effect of culturing antibody preparations with RML LVS. Antibodies (500 μ g/ml, immune or non-immune) were incubated with RML LVS for 30 minutes at 37°C with 5% CO₂. These slurries were then diluted out and enumerated on CHA plates. As is seen above, incubating bacteria with immune antibodies resulted in significantly lower titers than non-immune ($p = 0.0054$) and PBS ($p = 0.0044$) treated RML LVS when plated on agar (Brown-Forsythe ANOVA and Dunnett's multiple comparison tests). In contrast, there was no significant difference of RML LVS growth when incubated with the PBS control or non-immune antibodies ($p = 0.488$).

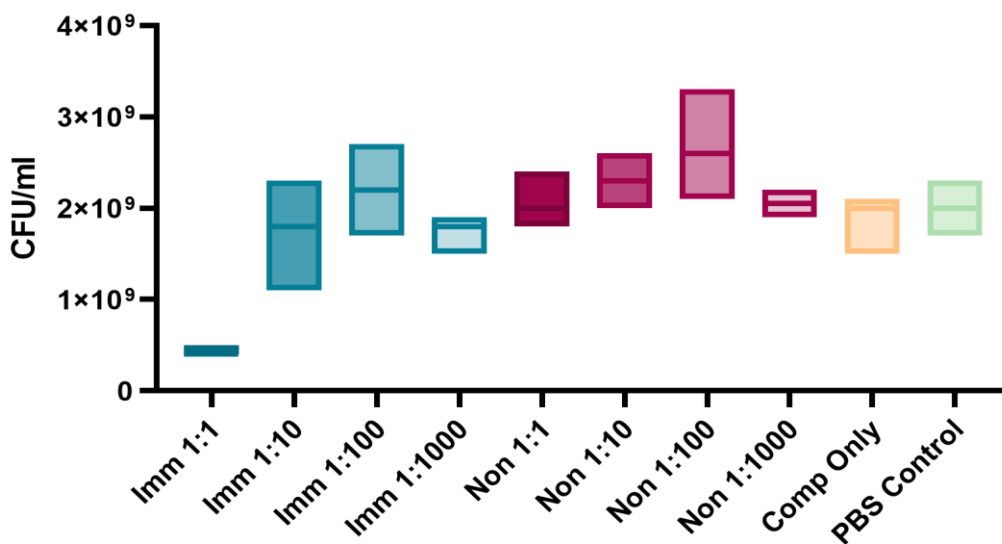


Figure 14. Complement-Mediated Killing of RML LVS with Antibodies.

Figure 14 shows the titers of RML LVS when mixed with different dilutions of rabbit complement. There was a slightly significant difference overall between titers (Brown-Forsythe ANOVA, $p = 0.0162$). However, there was no significant difference between any combination of complement and antibody when compared to either complement alone or PBS controls (Dunnett's Multiple Comparisons Tests). This is surprising because the immune antibody to complement 1:1 ratio exhibited about a 10-fold reduction in RML LVS titers. This experiment was performed once, so future work should also focus on repetition in order to confirm these findings.

4.2.2 Agglutination Tests

Table 5. Agglutination Titers of Hyperimmune and Non-Immune Antibodies

Antibody	Optimal Antigen Dilution	Agglutination Titer
Hyperimmune	1:4	1:640
Naïve	1:8	1:2

Table 5 shows the agglutination titers of hyperimmune and naïve purified antibodies from rabbits, respectively. It is important to note that these antibodies are standardized to a concentration of 500 µg/ml, while many other tests use undiluted sera or plasma. This could explain the relatively low agglutination titer of the immune sample compared to literature values (65, 66). The titer of the hyperimmune antibodies was 1:640 while the antibody titer for the naïve sample was 1:2. Additionally, the optimal antigen concentration was different for each sample. This may be due to the difference in balance of bacteria and antibody ratios needed to agglutinate the bacteria inside the space of the well. If the antigen concentration is normalized to the hyperimmune antibody sample, then the naïve sample would be negative. This experiment was performed twice, so future work may want to confirm results by repetition, especially with undiluted purified samples. In addition, future work will need to use the same antigen dilution for agglutination tests.

4.2.3 Infection Assays of J774s

Infection assays using the J774A.1 cell line often resulted in bacterial titers on all infection timepoints except for the initial timepoint (0 hr). The following results are therefore the products of the experiments that did manage to produce bacterial titers at all timepoints, albeit very low concentrations. More details concerning these experiments and their issues are in the discussion section.

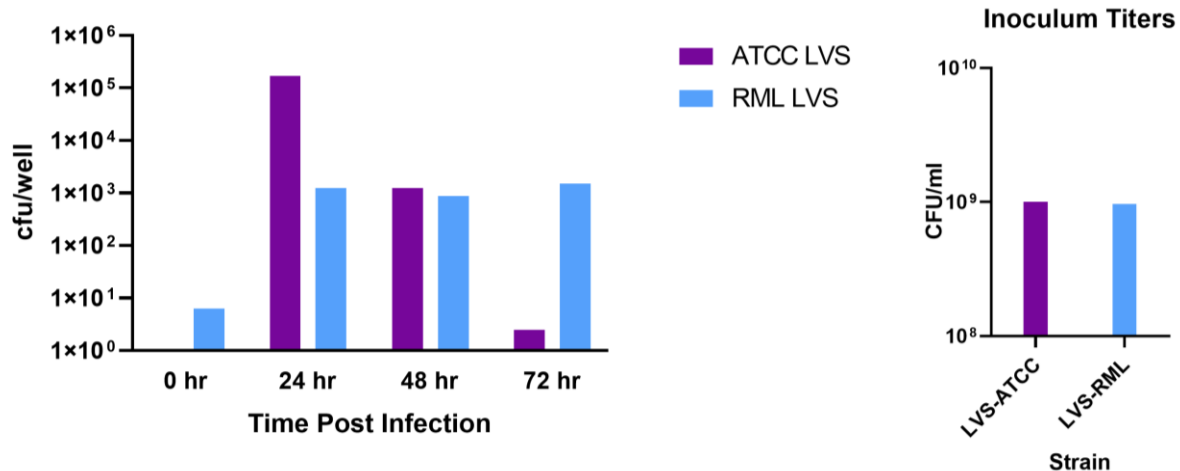


Figure 15. Comparison of AT C LVS strain and RML LVS straing during infection of J774 cells.

During initial experiments, it was suspected that the ATCC LVS strain used for infection assays had lost virulence and ability to infect J774 macrophages. **Figure 15** shows the intracellular growth of ATCC LVS (purple) and RML LVS (blue) over 72 hours. As can be seen above, the RML strain produced colonies during initial infection (0 hr) and sustained intracellular growth up to 72 hours. In contrast, the ATCC LVS strain did not produce colonies during the initial infection but peaked at 24 hours before decreasing at 48 and 72 hours post infection. Taken together, these data indicate that the RML LVS had better initial infection in cells in comparison to the ATCC LVS strain. However, ATCC LVS did replicate to higher titers at 24 and 48 hours post-infection while the RML LVS had overall less changes in replication from 24 to 72 hours after infection. This experiment was performed once. Based on these results, future infection assays and mouse experiments used the RML LVS strain instead of the ATCC LVS strain.

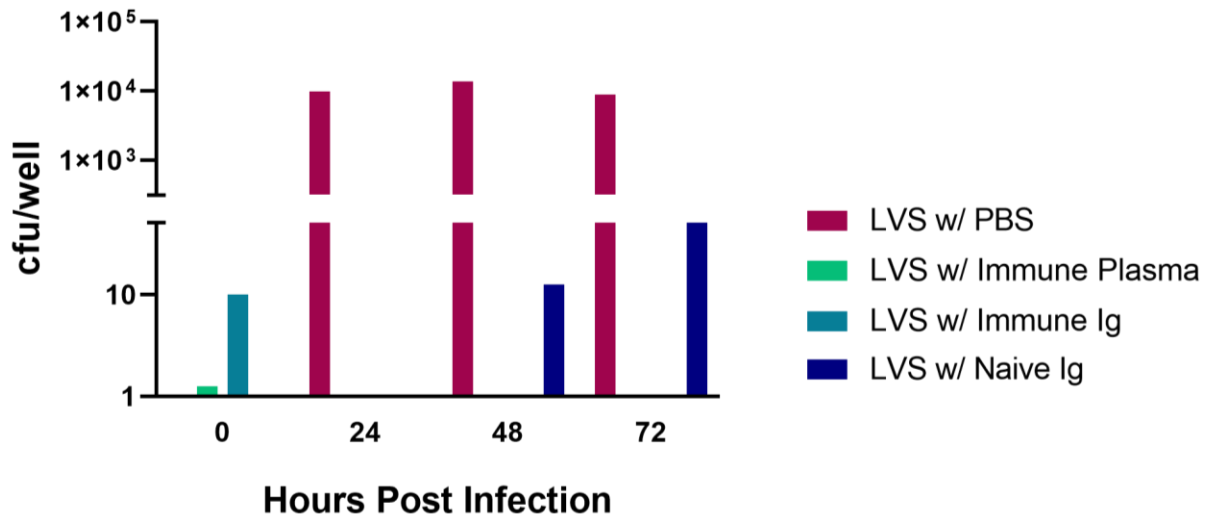


Figure 16. Effects of opsonization of RML LVS during infection with J774 cells.

The graph above shows an early infection assay using unpurified rabbit immune plasma as a positive control and non-immune purified antibodies and PBS as negative controls. In this infection, there was increase in the number of intracellular *Francisella* opsonized with immune antibodies either purified or non-purified. Additionally, *Francisella* incubated with non-immune antibodies appeared to stall intracellular growth until 48 hours post-infection. It is important to note that this experiment was one successful trial while many different trials failed. Additional repetitions of this experiment would be needed to verify these results.

4.3 Passive Protection from Lethal RML LVS Aerosol Infection in BALB/c Mice

4.3.1 Determining LD50 of RML LVS in Aerosol Infection of BALB/c Mice

4.3.1.1 Aerosol Dose

Table 6. Aerosol Summary for LD50 Determination

Target Dose (CFU)	Mice	Weight (g)	MV (ml)	[Nebulizer]	[AGI]	[Aerosol]	Spray Factor	Inhaled Dose
10	5	18.1	18.4	1.30E+06	2.60E+03	4.3E+02	3.3E-07	79.7
100	5	17.5	17.9	1.57E+07	1.17E+04	1.9E+03	1.2E-07	348.8
1,000	5	17.2	17.7	1.00E+08	4.27E+04	7.1E+03	7.1E-08	1,261.3

The table above summarizes the aerosol challenge of female BALB/c mice in order to determine lethal dose. The weights listed above are the average weight of all animals in each group. The respective target doses are shown on the left while the actual inhaled doses are shown in the last column on the right.

4.3.1.2 Survival Curve of BALB/c Mice

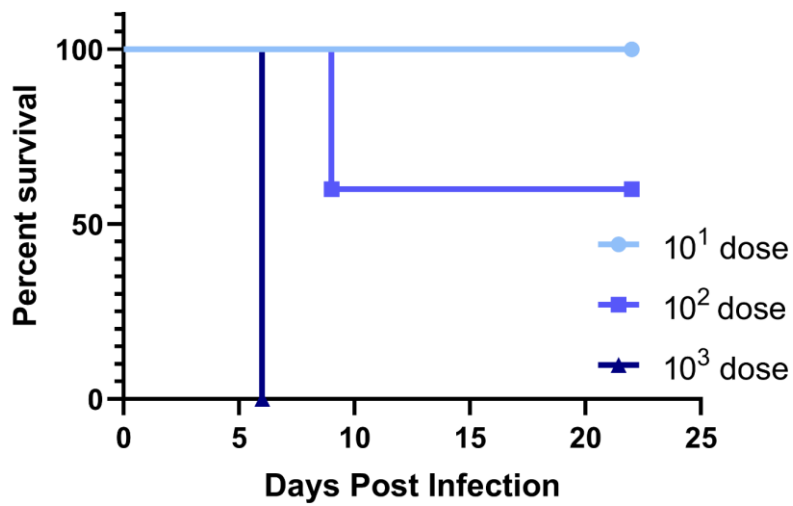


Figure 17. Survival of BALB/c mice with varying doses of aerosolized RML LVS.

The graph above shows the survival curve of different target doses in female BALB/c mice. Mice infected with the highest dose, approximately 1,000 CFUs, succumbed to infection around 6 days post-infection. In the group of animals infected with approximately 100 CFUs, about half the mice succumbed to infection while the others survived. All mice infected with approximately 10 CFUs survived infection.

4.3.1.3 Clinical Signs of Disease in BALB/c Mice

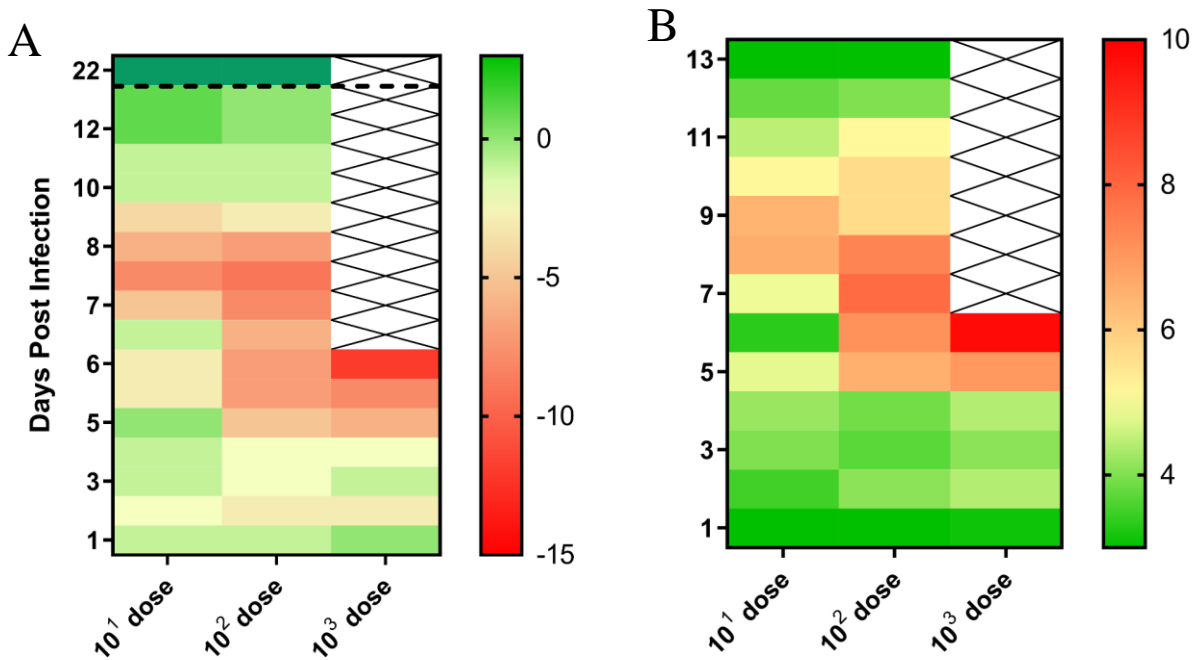


Figure 18. (A) Weight Loss and (B) Clinical Score of BALB/c Mice Infected with Different Doses of RML LVS.

Clinical signs and weight were monitored for 13 days after initial infection of RML LVS. Weight loss, shown on the left map, was more severe in mice infected with higher doses of bacteria. Additionally, onset of weight loss appeared later after infection in animals with lower doses. Clinical scores, shown on the right, were higher for animals with higher doses. Euthanasia criteria was reached in animals that succumbed to infection approximately six days after the aerosol. All animals that survived were back to baseline weights and scores by 13 days post-infection. Animals were sacrificed when the experiment ended after 22 days.

4.3.2 Comparison between Treatment Routes

4.3.2.1 Aerosol Dose

Table 7: Aerosol Summary for Determining Passive Immunization Route

	Mice	Weight (g)	MV (ml)	[Nebulizer]	[AGI]	[Aerosol]	Spray Factor	Inhaled Dose
i.p. Tx	30	18.8	19.0	2.37E+08	1.90E+04	3.2E+03	1.3E-08	600.3
i.n. Tx	30	18.4	18.6	2.37E+08	2.08E+04	3.5E+03	1.5E-08	644.0

The table shown above summarizes the dose calculations for the aerosol challenge of BALB/c mice. This experiment was designed to determine if there were significant differences in the route of antibody administration. The difference in the doses shown above is minimal, leading to similar experimental design.

4.3.2.2 Survival Curve of BALB/c Mice

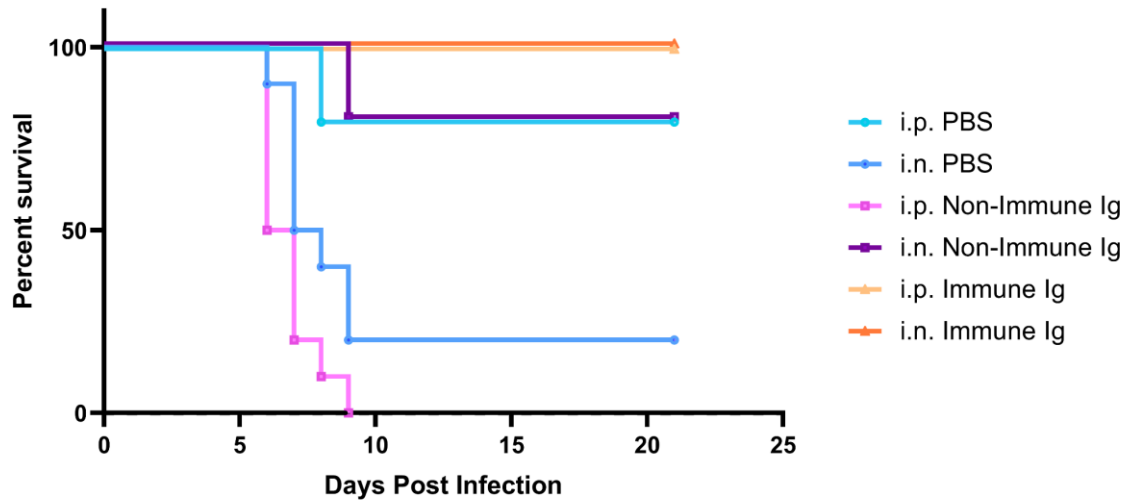


Figure 19. Survival Curve of BALB/c Mice Passively Immunized Either i.n. or i.p.

This graph shows the survival curve of all treatment groups of animals passively immunized with PBS, non-immune antibodies, or immune antibodies delivered either intranasally or intraperitoneally. In either route, the animals immunized with hyperimmune antibodies survived infection while at least 20% of control animals groups succumbed to infection. Interestingly, animals inoculated with non-immune antibodies via i.p. route all succumbed to infection while animals inoculated with the same non-immune antibodies via i.n. route had 80% survival (Log-rank test, $p < 0.0001$). The opposite effect was seen in animals inoculated with the PBS control; 80% of animals succumbed to infection when inoculated i.n., but only 20% succumbed when inoculated via i.p. route. This difference was found to be significantly different (Log-rank test, $p = 0.0060$).

4.3.2.3 Weight Loss of BALB/c Mice

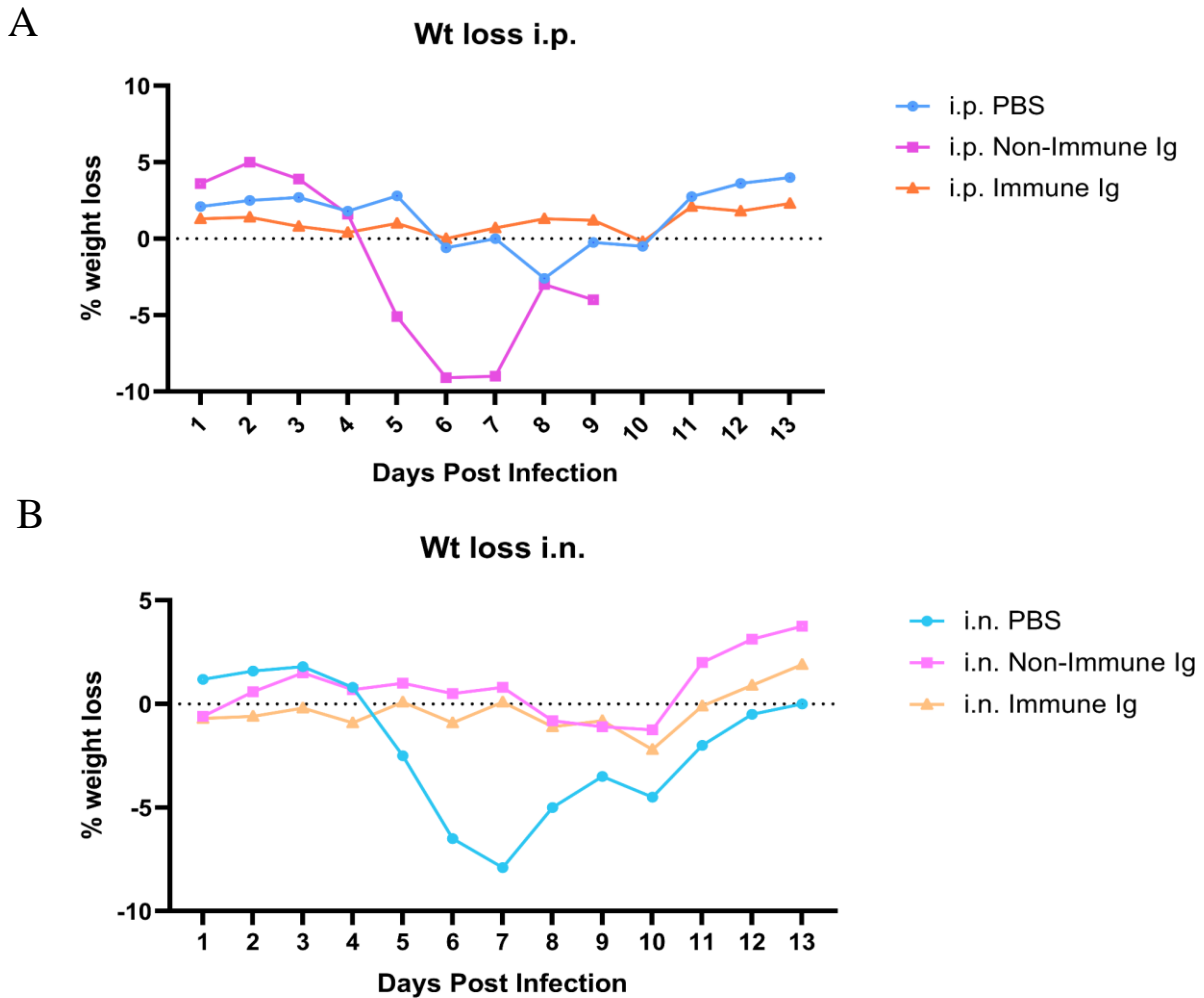


Figure 20. Weight Loss of BALB/c Mice Immunized via Different Routes.

Weight loss graphs were separated out based on immunization route. The top graph, (A), shows all groups immunized through the intraperitoneal route and the bottom graph, (B), shows all groups immunized through the intranasal route. The weight loss of either group corresponds to the survival curves in that animals who succumbed to infection lost more weight than animals that survived. In the top graph, animals in the non-immune antibody control group lost more weight than either the PBS control group or the immune antibody group. In the bottom graph, the PBS

control group lost more weight than the non-immune control group or the immune group. This trend was seen in all animals of the group (n=10). In both graphs, the most severe weight loss was observed around 6-7 days post infection and increased over the next few days until symptoms disappeared.

4.3.2.4 Tissue-Specific Bacterial Burden in BALB/c Mice

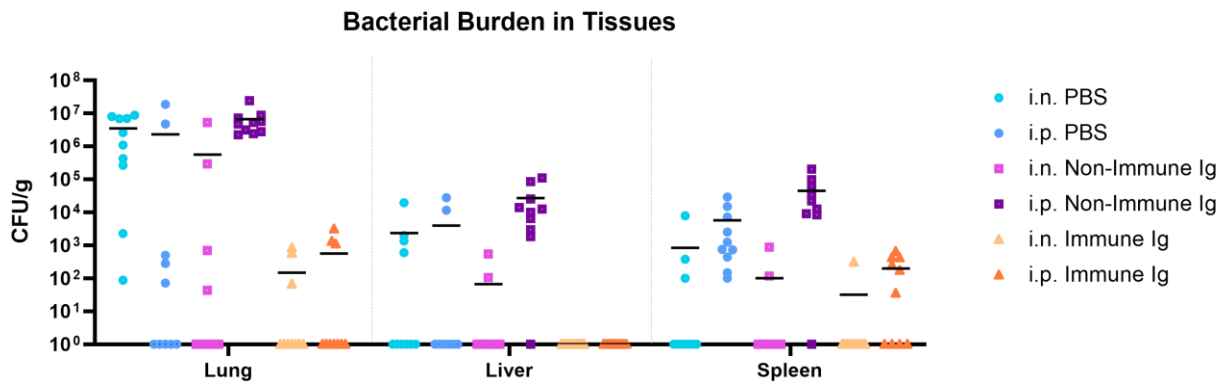


Figure 21. Bacterial Titers in the Lungs, Livers, and Spleens of BALB/c Mice Passively Immunized i.p. or i.n.

The differences in bacterial burden among animals are seen in the graph above. There is a significant difference between treatment groups (2-way ANOVA, $p = 0.0120$), but this difference only accounts for 8.4% of the total variation seen between animals. Mice inoculated with immune antibodies of either route showed slightly less bacterial burden in tissues than any control groups. However, this difference was not statistically significant, probably due to the high deviation between values (Tukey's tests). Bacterial titers in the lungs and livers were lower in the surviving animals than in animals that succumbed to infection. Bacterial titers in the spleens of the animals were not different between survivors and non-survivors.

4.3.3 High-Dose Challenges

The following experimental design was repeated twice since the first trial had an overwhelmingly high dose. Since the doses are different by approximately a log, the results could not be combined onto one graph.

4.3.3.1 Aerosol Dose

Table 8. Aerosol Summary for High-Dose RML LVS Challenge in Mice - Trial 1.

Mice	Weight (g)	MV (ml)	[Nebulizer]	[AGI]	[Aerosol]	Spray Factor	Inhaled Dose
30	18.06	18.40	8.03E+09	3.77E+06	6.28E+05	7.82E-08	1.15E+05

Table 9. Aerosol Summary for High-Dose RML LVS Challenge in Mice - Trial 2.

Mice	Weight (g)	MV (ml)	[Nebulizer]	[AGI]	[Aerosol]	Spray Factor	Inhaled Dose
30	17.40	17.90	1.17E+09	8.10E+05	1.4E+05	1.16E-07	2.42E+04

The two tables shown above summarize the aerosol challenges of RML LVS in BALB/c mice. Animals were passively immunized approximately 24 hours prior to challenge. In trial 1, the calculated inhaled dose is approximately 10-fold higher than in trial 2.

4.3.3.2 Survival Curve of BALB/c Mice

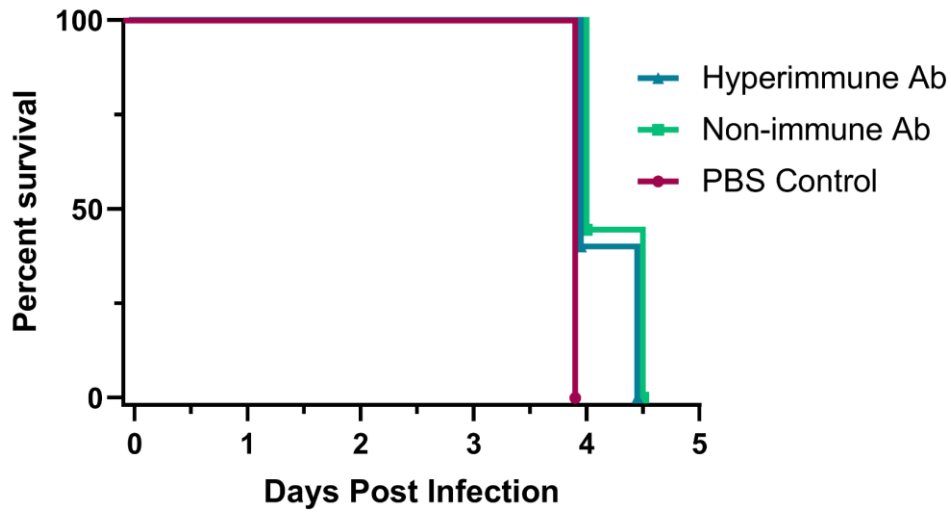


Figure 22. Survival Curve of Passively Immunized BALB/c Mice Challenged with RML LVS – Trial 1.

All animals (n=10/group) in challenge trial 1 succumbed to infection around 4-4.5 days after the aerosol. There was no significant difference seen between the survival of groups (Log-rank test, $p = 0.059$). All animals in the PBS control group succumbed to infection after 4 days, while about half of the immune and non-immune groups succumbed. However, by 4.5 days after infection, all remaining animals met euthanasia criteria.

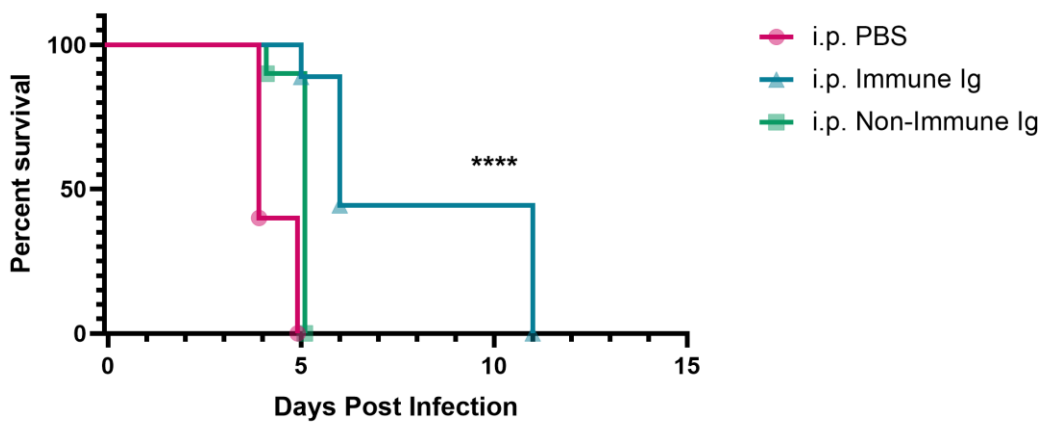


Figure 23. Survival Curve of Passively Immunized BALB/c Mice Challenged with RML LVS – Trial 2.

BALB/c mice (n=10/group) challenged with a dose 10-fold lower than the animals in trial 1 demonstrated a different pattern of survival. In this experiment, about half of the animals that were administered hyperimmune antibodies had a significant extension of time to death (Logrank test for trend, $p < 0.0001$).

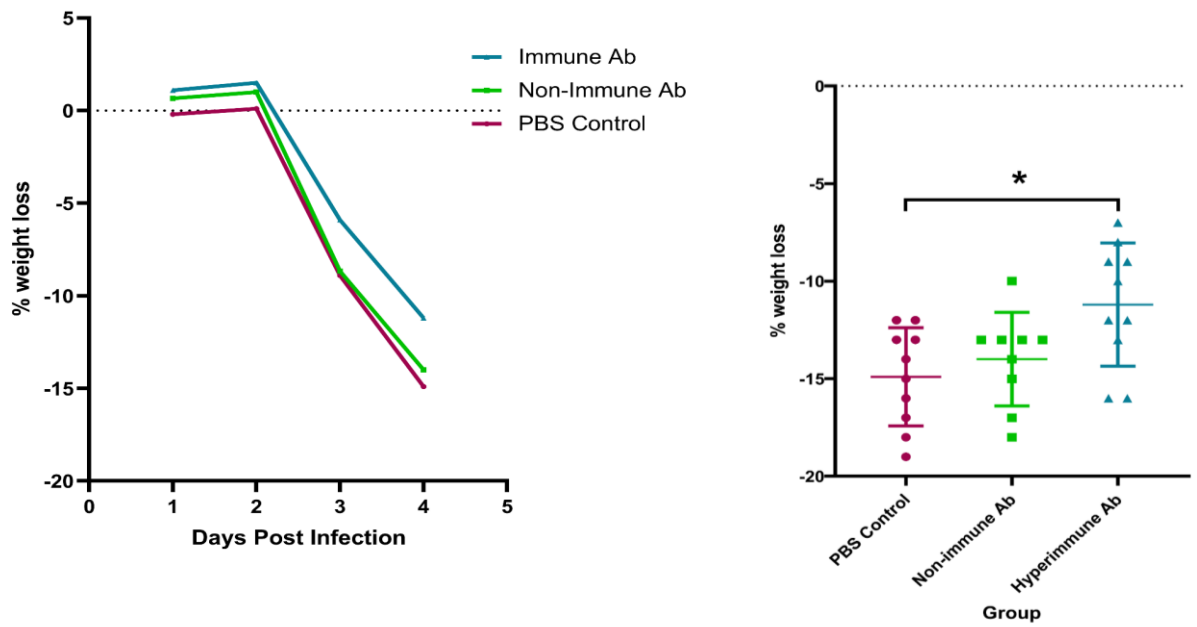


Figure 24. Weight Loss of BALB/c Mice after Aerosol Challenge, (A) Over Time and (B) on Day 4 Post Infection.

4.3.3.3 Weight Loss of BALB/c Mice

Weight loss of animals challenged with 10^5 CFU of aerosolized RML LVS exhibited profound weight loss leading up to death (**Figure 24A**). However, on 4 days after infection, animals immunized with hyperimmune antibodies showed significantly less weight loss than the PBS control group (Tukey's test, adjusted $p = 0.014$). There was a slight difference in weight loss between immune and non-immune antibodies (Tukey's test, adjusted $p = 0.83$).

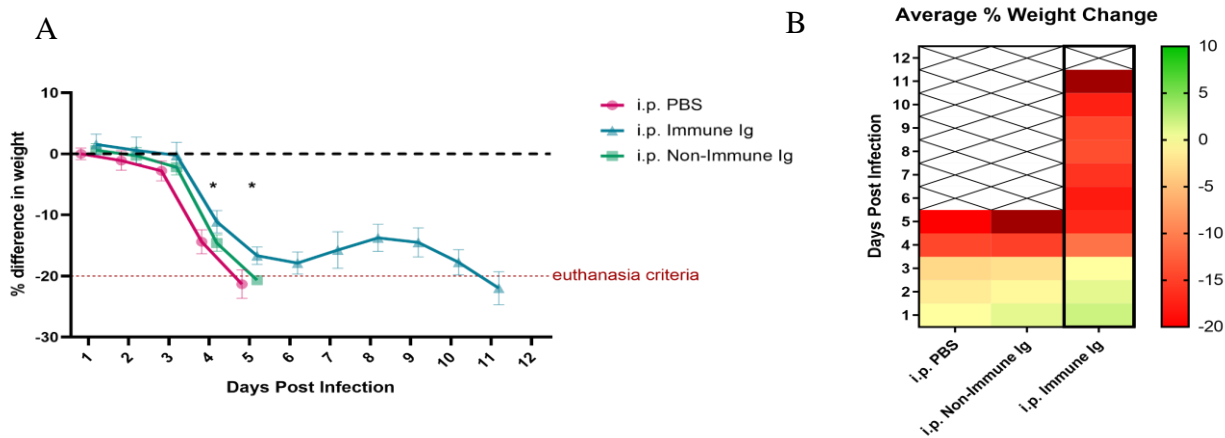


Figure 25. Weight loss of passively immunized BALB/c mice after high-dose aerosol challenge of RMS LVS.

Mice challenged with a dose 10-fold less than before still lost a large amount of weight after 4 days (**Figure 25**). Unlike the first trial, animals given hyperimmune antibodies lost significantly less weight than PBS on days 1 ($p = 0.042$), 3 ($p = 0.024$), 4 ($p = 0.0076$), and 5 ($p = 0.0076$) after challenge. Hyperimmune animals also lost significantly less weight than non-immune antibody groups on days 4 ($p = 0.00073$) and 5 ($p = 0.000005$) after challenge. Taken together, these data indicate that there were larger differences seen when comparing the hyperimmune antibody treated animals with PBS controls compared to the non-immune antibody controls. This could be due to non-immune antibodies playing a role in mitigating disease in mice compared to the PBS control, although this difference was not significant. All reported statistics were t-tests performed in GraphPad.

4.3.3.4 Tissue-Specific Bacterial Burden in BALB/c Mice

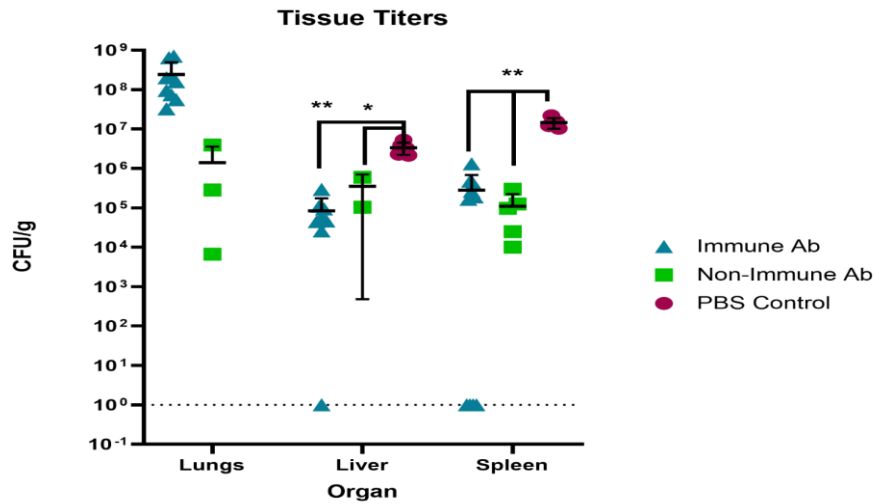


Figure 26. Bacterial burden in immunized BALB/c mice challenged with high-dose RML LVS.

Bacterial burdens of animals challenged with the highest dose of RML LVS are shown in **Figure 26**. The bacteria in the lungs of the PBS control group were unable to be enumerated; bacteria titers were not diluted enough, and samples were discarded. Bacterial burden between immune and non-immune groups was not significantly different in any of the tissues. However, both the non-immune and immune animals had significantly less bacterial burden than the PBS group in the liver and spleen (t-test). This trend would likely also be seen in the lungs, since the bacterial burden was too high to be counted. * $p < 0.05$, ** $p < 0.001$

5.0 Discussion

5.1 Plasma Purification

The novelty of this work is that I purified antibodies from plasma in order to create a protein mix that was relatively purer than plasma alone and contained a known amount of protein in the solution. There have been numerous studies examining the effects of injecting serum or plasma into different animals in order to try to confer protection against tularemia, with mixed results (see **Table 1**). Other studies examined monoclonal antibodies, but no one has yet to look at a purified polyclonal antibody solution that we have examined here. It was my hope that the purification method I used would be suitable for concentration of antibody and removal of other proteins, generating a material useful for evaluating the role of antibody in protection against tularemia. Purification and concentration of antibody has not been previously attempted in studies evaluating the role of antibody in protection against tularemia (31), (see **Table 1**). Using a combination of standard antibody biochemistry protocols (57, 58), I was able to achieve an affordable method to crudely purify antibody out of plasma for use in preliminary research. If this therapeutic was to be further tested for use in humans, a more refined purification method would be desirable (such as a column).

My experiments indicate that 43% ammonium sulfate solution was optimal for purifying and precipitating out rabbit antibodies. When the purification products were normalized by total protein concentration (500 $\mu\text{g/ml}$), large differences were seen in the EC50 curves for IgG. Purified rabbit antibodies resulting from the 33% or 43% saturated ammonium sulfate had an overall higher avidity than the other products of the purification process. It should be noted that each product of

the purification process had remnants of antibody in the solution, as indicated by the EC50 titration curves. This means that during each step in our process, there was some loss of antibody. This is consistent with reports in the literature for antibody purification and concentration using these methods. In future studies, this process could be refined further to minimize this loss, such as using affinity columns

5.2 In vitro Effects of Antibody on *F. tularensis* RML LVS

Phagocytosis is a key event during the *Francisella* life cycle in a mammalian host (17). Studies examining opsonization of *Francisella* with serum found that the FcγR and C3R may dictate the route of the intracellular bacteria after uptake (38). While not fully understood, it is thought that opsonization by serum or complement redirect *Francisella* bacteria to pathways that may initially result in bacterial killing. Opsonization experiments in this work focused on changes in bacterial growth extracellularly through changes in titers and intracellularly through infection assays. Mixing LVS bacteria with antibodies resulted in significantly reduced titers of bacteria when grown on CHA plates, as is shown in **Figure 13**. This is likely due to the clustering of bacteria through agglutination, as seen in **Table 5**. It could also be due to direct killing of the bacteria by antibodies, although this was not tested. Many groups have found that complement does not cause bacterial killing in *F. tularensis* (36, 38, 67). Complement protein C3 mediates bacterial uptake into phagocytes, but the cascade does not continue to form the attack complex (67). This finding was further confirmed based on the results of **Figure 14**, which shows that there was no difference between the bacterial titers of RML LVS when complement was added, even

though the 1:1 ratio had approximately a 10-fold decrease in bacterial titers. This experiment was performed once, so in future work these results should be confirmed through repetition.

Intracellular growth was extremely difficult to characterize in J774 cells, as is discussed in more detail later in this section. The one infection assay that did result in growth at all time points is shown in **Figure 16**. This experiment used a high concentration of purified antibody from both naïve rabbits and hyperimmune rabbits. Additionally, unpurified regular immune plasma was used as a positive control. Based on the results of this assay, there was an increase in initial uptake of bacteria by J774s as seen in the increase of titer at 0 hours post-infection. At later timepoints, though, immune plasma and antibodies caused observed death of the J774s (not shown) and reduced titers of LVS on CHA plates.

Infection assays using J774A.1 macrophage-like cells were largely unsuccessful despite numerous efforts. The main issue was detecting bacteria inside cells shortly after initial infection, approximately 3-4 hours after LVS slurries were first added to cell monolayers. This timing was dependent on pipetting skills during the wash steps of the assay, which was time-consuming and dependent on the number of plates used in the assay. Undetectable levels of LVS resided inside the macrophages, which were later detected by higher titers at later time points. This was particularly confusing because this assay has worked for other groups (68-70) and previous members of the Reed lab. During initial experiments, it was thought that the original ATCC LVS stock we used was becoming damaged in some way during the freeze-thaw process. Thus, we decided to create a stock of RML LVS sent to the Reed lab from colleagues at Rocky Mountain Labs. **Figure 15** shows a successful infection assay comparing the intracellular growth between the RML LVS biovar and the ATCC LVS biovar. Based on this assay, it appeared that RML LVS was more successful at infecting J774 cells than the ATCC LVS, as indicated by the relative titers

at 0 hours post-infection. During the 24-hour timepoint, RML LVS did not produce as high of a titer as the ATCC LVS. However, the ATCC LVS biovar peaked at 24-hours post-infection before dramatically decreasing at 48- and 72-hours post-infection. These data indicate that while the RML LVS did not grow to as high of a titer as the ATCC LVS, it did produce a more sustained infection in the macrophage-like cells. This is important because it may relate to the pathogenesis of RML LVS seen in mice during later experiments.

5.3 Passive Immunization of BALB/c Mice Against Aerosolized RML LVS

The mouse experiments in this work were performed using the RML LVS biovar of *Francisella tularensis* subsp. *holarctica*. This strain was chosen because it has been shown to be more virulent in mice than the ATCC LVS (4), leading to a more stringent challenge. Additionally, RML LVS has not yet been used in aerosol infections of BALB/c mice before, so we were also interested to see the differences between this biovar and the ATCC biovar. Mice without any treatment succumbed to infection about 4-5 days after infection, which was similar to previous work in the Reed lab (62). However, the LD50 and LD99 of RML LVS was approximately 10-fold lower than the ATCC biovar used previously. It should be taken into consideration that LVS of either biovar is not as translatable as virulent type A or B strains and that mice are not as translatable to humans as other models. Mice are more susceptible to *Francisella* infections, and while an infection with LVS may not cause disease in humans, it can be a lethal infection in mice. Thus, while antibodies alone did not protect mice from lethal infections, these experiments should be repeated in the rabbit model. In other studies (see **Table 1**), antibodies alone have not protected

mice from infection with the fully virulent Schu S4 strain. On the other hand, rats have been successfully passively immunized against Schu S4 (71).

The route of administration of immune antibodies did not appear to make a difference in survival or bacterial burden in BALB/c mice (**Figures 19-21**). It was surprising that the i.p. non-immune antibody group succumbed to infection while the i.n. non-immune antibody group had 80% survival. This may be due to the biological route of infection, since antibodies may have remained localized in the respiratory tract on the day of infection. In these areas of the body, the non-immune antibodies may have had some non-specific binding to *F. tularensis*, allowing the animals to control infection better than the PBS control. However, PBS administered i.p. resulted in 80% survival, while PBS administered i.n. resulted in 20% survival. It is unlikely that the treatment groups were switched at any time during the experiment due to human error. While unlikely, maybe the i.p. PBS provided extra fluids to the animals before infection, serving as some sort of pre-exposure supportive care while PBS delivered i.n. deposited excess fluid in the lungs, becoming a co-morbidity in these animals. It is more likely though that the low challenge dose had some unexpected effects on the differences in survival, making it impossible to interpret these results.

Animals treated with immune Ab and challenged with 2.42×10^5 CFU of RML LVS had a significant extension of time to death by about 6 days. When animals were challenged with a bacterial dose 10-fold higher, there was no significant extension in time to death, although animals in the immune group did lose significantly less weight than the PBS control group on day of euthanasia. Bacterial burden of animals in the PBS control group were significantly higher in the spleens and livers compared to the antibody groups. These data suggest that a single bolus of antibody may control the infection for a short time but cannot offer full protection. This supports

the idea that hyperimmune antibodies were able to prevent *F. tularensis* from disseminating from the lungs of at least a few mice. Additionally, similar results were seen in the bacterial burdens of animals challenged with sub-lethal doses, although these results were not significant.

Overall, the data in these experiments indicate that antibodies do play a role in protection against tularemia, as seen by the differences in weight loss, bacterial burden, and time to death. However, antibodies in a single inoculation were not sufficient to fully protect BALB/c mice against aerosolized *F. tularensis* infection at high challenge doses. Antibody seems to function by binding to *F. tularensis* in the body, increasing uptake in macrophages. Studies by other groups indicate that this uptake is modified by the opsonizing condition of the bacteria *in vitro* (38) and *in vivo* (36). This process and subsequent bacterial killing is not dependent on complement (36), although future work should confirm these results since the experiment was performed once in this work.

5.4 Importance

Currently, there is no licensed vaccine to protect against tularemia. Since this disease is rare, there are ethical and resource barriers in vaccine development. It would be logistically difficult to conduct trials of any vaccines in humans, so the main route of licensure many researchers go by is using the FDA Animal Rule. According to this rule, the exact mechanisms of protection elicited by a candidate vaccine must be characterized in order to further proceed in the licensure process (28). Our lab has previously examined multiple live vaccine candidates in the rabbit model, which offers a more human-like clinical presentation of disease (8). This work provides further insight into the debated role of antibody in vaccine-elicited protection from

virulent *F. tularensis* strain Schu S4. Taken together, we have shown that antibodies produced in these hyperimmune rabbits had high avidity to Schu S4 bacteria, resulting in higher binding and a reduction in bacterial titers when grown on CHA plates. These antibodies did not provide complete protection in the mouse model, indicating that while antibodies may be important, they are not a sole mechanism of protection. However, future work should confirm this by assessing whether multiple injections of antibody over time might confer protection in mice. Numerous other studies indicate that cellular immunity is important for protection against intracellular bacteria such as *Francisella*, while antibodies have been thought to play no role at all. However, this work supports the findings that while antibodies may not be protective alone, they do play a role in the immune response to *Francisella* species.

Appendix Supplemental Tables and Figures

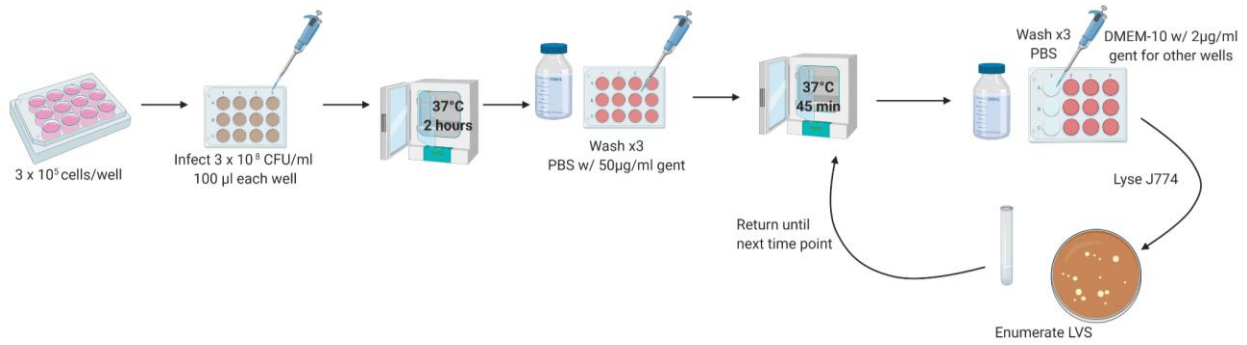


Figure 27. Infection Assay Schematic

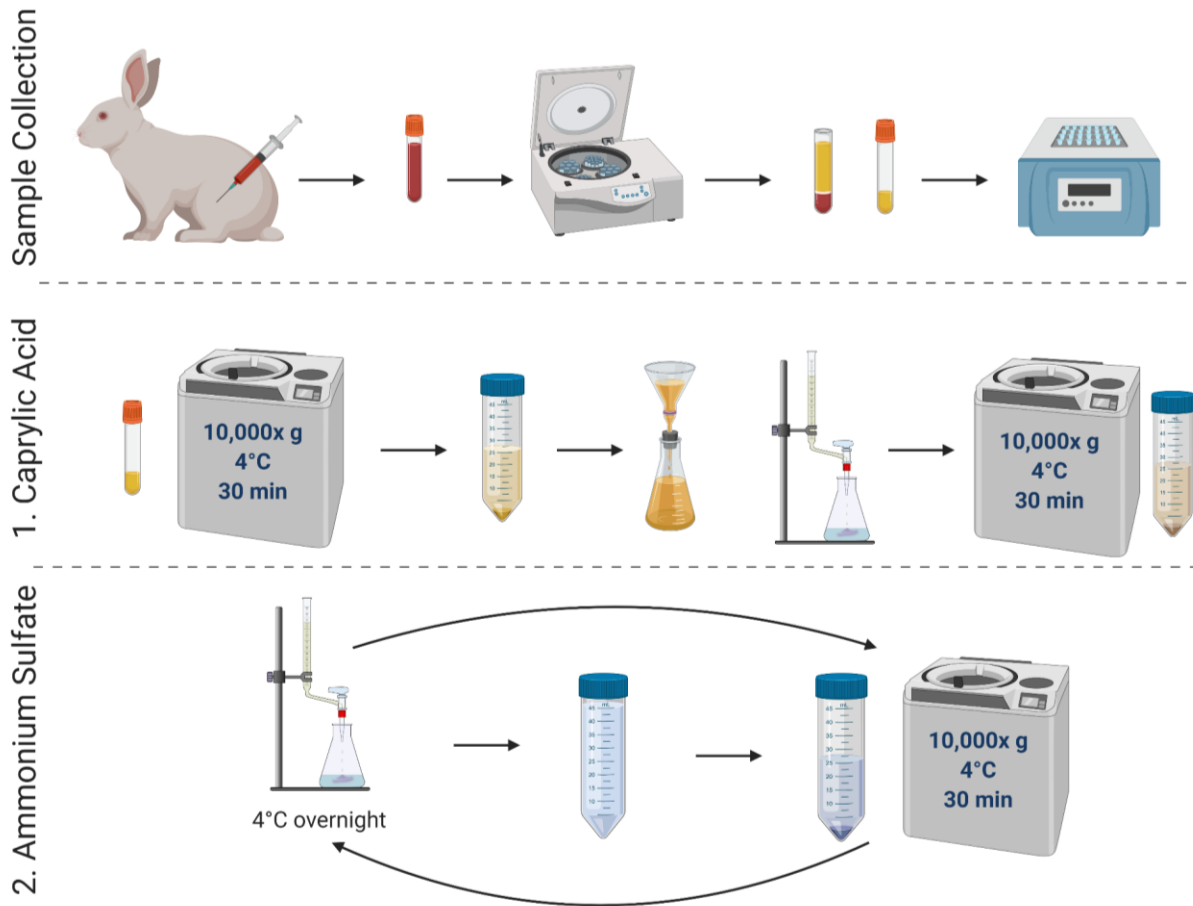


Figure 28. Purification of Antibody Schematic.

Table 10. ELISA Values of Optimization of Plasma Purification.

	Positive Control	Negative Control	plasma	Caprylic Acid ppt	33% (NH₄)₂SO₄ ppt	43%(NH₄)₂SO₄ ppt	43% (NH₄)₂SO₄ Supernatent
Max RLU_s	8740000	167000	7080000	6890000	6620000	6280000	3750000
EC50	10250	67.24	580.3	1070	10538	13554	~ 544.8
Log EC50	4.011	1.828	2.764	3.029	4.023	4.132	~ 2.736
r² value	0.9591	0.8313	0.9906	0.9829	0.9129	0.9466	0.8693

Table 11. ELISA Values of Hyperimmune Plasma Purification Products.

	Positive Control	Negative Control	Unfiltered Plasma	Filtered Plasma	Plasma pellet	Caprylic Acid ppt	IgG Pellet	43% (NH₄)₂SO₄ Supernatent
Max RLU_s	8740000	167000	4700000	15000	6510000	691000	6180000	3370000
EC50	10250	67.24	2652	239.7	611.1	12969	6011	4312
Log EC50	4.011	1.828	3.424	2.380	2.786	4.113	3.779	3.635
r² value	0.9591	0.8313	0.9108	0.1539	0.9917	0.4326	0.9329	0.7965

Table 12. ELISA Values of Naïve Rabbit Plasma Purification Products.

	Positive Control	Negative Control	Unfiltered Plasma	Filtered Plasma	Plasma pellet	IgG Pellet	43% (NH₄)₂SO₄ Supernatent
Max RLU_s	8740000	167000	203000	229000	175000	192000	102000
EC50	10250	67.24	7.091	~ 17.36	~ 102.0	~ 33.88	~ 510.1
Log EC50	4.011	1.828	0.8507	~ 1.240	~ 2.009	~ 1.530	~ 2.708
r² value	0.9591	0.8313	**	0.9950	0.9732	0.8775	0.6063

** - GraphPad software unable to calculate r² value

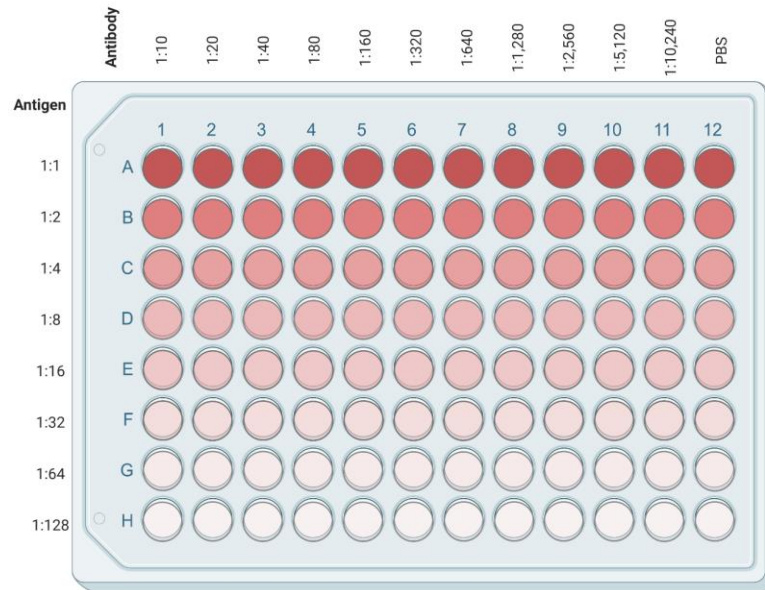


Figure 29. Agglutination Schematic Showing Antibody and Antigen Dilutions.

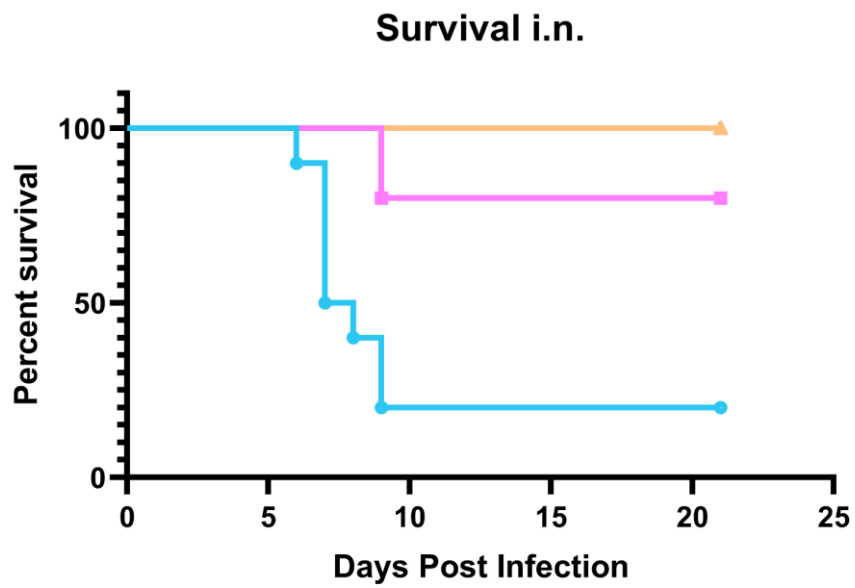


Figure 30. Survival of i.n. Treated Mice Only.

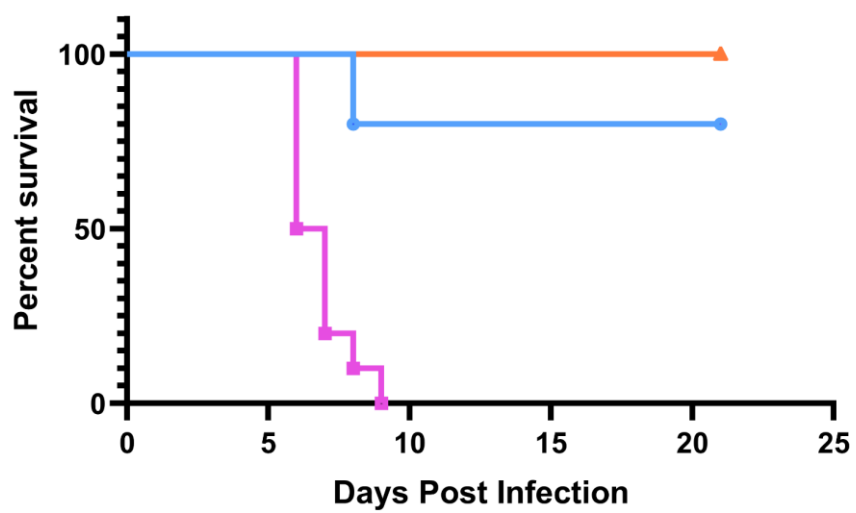


Figure 31. Survival of i.p. Treated Mice Only.

Bibliography

1. Hirschmann JV. 2018. From Squirrels to Biological Weapons: The Early History of Tularemia. *The American Journal of the Medical Sciences* 356:319-328.
2. Hofmann J. 2012. 93 - Tularemia, p 567-572. In Jong EC, Stevens DL (ed), *Netter's Infectious Diseases* doi:<https://doi.org/10.1016/B978-1-4377-0126-5.00093-8>. W.B. Saunders, Philadelphia.
3. Sunagar R, Kumar S, Franz BJ, Gosselin EJ. 2016. Tularemia vaccine development: paralysis or progress? *Vaccine (Auckland, NZ)* 6:9-23.
4. Griffin AJ, Crane DD, Wehrly TD, Bosio CM. 2015. Successful Protection against Tularemia in C57BL/6 Mice Is Correlated with Expansion of *Francisella tularensis*-Specific Effector T Cells. *Clinical and Vaccine Immunology* 22:119-128.
5. Klimpel GR, Eaves-Pyles T, Moen ST, Taormina J, Peterson JW, Chopra AK, Niesel DW, Carness P, Haithcoat JL, Kirtley M, Nasr AB. 2008. Levofloxacin rescues mice from lethal intra-nasal infections with virulent *Francisella tularensis* and induces immunity and production of protective antibody. *Vaccine* 26:6874-6882.
6. Gallagher-Smith M, Kim J, Al-Bawardy R, Josko D. 2004. *Francisella tularensis*: Possible Agent in Bioterrorism. *American Society for Clinical Laboratory Science* 17:35-39.
7. Control CfD. December 13, 2018 2018. Tularemia: Diagnosis and Treatment, *on Centers for Disease Control*. <https://www.cdc.gov/tularemia/diagnosistreatment/index.html>. Accessed
8. Reed DS, Smith LK, Dunsmore T, Trichel A, Ortiz LA, Cole KS, Barry E. 2011. Pneumonic Tularemia in Rabbits Resembles the Human Disease as Illustrated by Radiographic and Hematological Changes after Infection. *PLOS ONE* 6:e24654.
9. Anonymous. 2002. *Public Health Security and Bioterrorism Preparedness and Response Act*. Washington DC.
10. Christopher LGW, Cieslak LTJ, Pavlin JA, Eitzen EM, Jr. 1997. Biological Warfare: A Historical Perspective. *JAMA* 278:412-417.
11. Feldman KA, Ensore RE, Lathrop SL, Matyas BT, McGuill M, Schriefer ME, Stiles-Enos D, Dennis DT, Petersen LR, Hayes EB. 2001. An Outbreak of Primary Pneumonic Tularemia on Martha's Vineyard. *New England Journal of Medicine* 345:1601-1606.
12. Ellis J, Oyston PCF, Green M, Titball RW. 2002. Tularemia. *Clinical Microbiology Reviews* 15:631-646.
13. Anonymous. Dec 11, 2019 2019. Tularemia: Statistics. Accessed March 1.
14. Hajjar AM, Harvey MD, Shaffer SA, Goodlett DR, Sjöstedt A, Edebro H, Forsman M, Byström M, Pelletier M, Wilson CB, Miller SI, Skerrett SJ, Ernst RK. 2006. Lack of In Vitro and In Vivo Recognition of *Francisella tularensis* Subspecies Lipopolysaccharide by Toll-Like Receptors. *Infection and Immunity* 74:6730-6738.
15. Celli J, Zahrt TC. 2013. Mechanisms of *Francisella tularensis* intracellular pathogenesis. *Cold Spring Harbor perspectives in medicine* 3:a010314-a010314.

16. Schmitt DM, Barnes R, Rogerson T, Haught A, Mazzella LK, Ford M, Gilson T, Birch JWM, Sjöstedt A, Reed DS, Franks JM, Stolz DB, Denvir J, Fan J, Rekulapally S, Primerano DA, Horzempa J. 2017. The Role and Mechanism of Erythrocyte Invasion by *Francisella tularensis*. *Frontiers in cellular and infection microbiology* 7:173-173.
17. Celli J, Zahrt TC. 2013. Mechanisms of *Francisella tularensis* intracellular pathogenesis. *Cold Spring Harb Perspect Med* 3:a010314.
18. Clemens DL, Lee B-Y, Horwitz MA. 2004. Virulent and Avirulent Strains of *Francisella tularensis* Prevent Acidification and Maturation of Their Phagosomes and Escape into the Cytoplasm in Human Macrophages. *Infection and Immunity* 72:3204-3217.
19. Santic M, Molmeret M, Klose KE, Abu Kwaik Y. 2006. *Francisella tularensis* travels a novel, twisted road within macrophages. *Trends in Microbiology* 14:37-44.
20. Wehrly TD, Chong A, Virtaneva K, Sturdevant DE, Child R, Edwards JA, Brouwer D, Nair V, Fischer ER, Wicke L, Curda AJ, Kupko III JJ, Martens C, Crane DD, Bosio CM, Porcella SF, Celli J. 2009. Intracellular biology and virulence determinants of *Francisella tularensis* revealed by transcriptional profiling inside macrophages. *Cellular Microbiology* 11:1128-1150.
21. Cowley SC, Elkins KL. 2011. Immunity to *Francisella*. *Front Microbiol* 2:26.
22. Gillette DD, Curry HM, Cremer T, Ravneberg D, Fatehchand K, Shah PA, Wewers MD, Schlesinger LS, Butchar JP, Tridandapani S, Gavrillin MA. 2014. Virulent Type A *Francisella tularensis* actively suppresses cytokine responses in human monocytes. *Frontiers in Cellular and Infection Microbiology* 4.
23. Schwartz JT, Barker JH, Long ME, Kaufman J, McCracken J, Allen L-AH. 2012. Natural IgM Mediates Complement-Dependent Uptake of *Francisella tularensis* by Human Neutrophils via Complement Receptors 1 and 3 in Nonimmune Serum. *The Journal of Immunology* 189:3064-3077.
24. Mares CA, Ojeda SS, Morris EG, Li Q, Teale JM. 2008. Initial Delay in the Immune Response to *Francisella tularensis* Is Followed by Hypercytokinemia Characteristic of Severe Sepsis and Correlating with Upregulation and Release of Damage-Associated Molecular Patterns. *Infection and Immunity* 76:3001-3010.
25. O'Malley KJ, Bowling JD, Barry EM, Hazlett KRO, Reed DS. 2019. Development, Characterization, and Standardization of a Nose-Only Inhalation Exposure System for Exposure of Rabbits to Small-Particle Aerosols Containing *Francisella tularensis*. *Infect Immun* 87.
26. Conlan JW, Chen W, Bosio CM, Cowley SC, Elkins KL. 2011. Infection of mice with *Francisella* as an immunological model. *Current protocols in immunology* Chapter 19:Unit-19.14.
27. De Pascalis R, Mittereder L, Chou AY, Kennett NJ, Elkins KL. 2015. *Francisella tularensis* Vaccines Elicit Concurrent Protective T- and B-Cell Immune Responses in BALB/cByJ Mice. *PloS one* 10:e0126570-e0126570.
28. Research CfDEaRCfBEa. 2009. Product Development Under the Animal Rule. FDA-2009-D-0007. Administration FaD,
29. Saslaw S, Carhart S. 1961. Studies with Tularemia Vaccines in Volunteers. III. Serologic Aspects following Intracutaneous or Respiratory Challenge in Both Vaccinated and Nonvaccinated Volunteers. *American Journal of Medical Sciences* 241:689-99.

30. Kadull PJ, Reames HR, Coriell LL, Foshay L. 1950. Studies on Tularemia. V. Immunization of Man. *The Journal of Immunology* 65:425-435.
31. Kenneth Murphy CWwcbAM, Leslie Berg, David Chaplin ; with acknowledgment to Charles A. Janeway Jr., Paul Travers, Mark Walport. 2016. *Janeway's Immunobiology*, 9th ed. Garland Science; Taylor & Francis Group, LLC, New York, NY.
32. Roberts LM, Powell DA, Frelinger JA. 2018. Adaptive Immunity to *Francisella tularensis* and Considerations for Vaccine Development. *Frontiers in cellular and infection microbiology* 8:115-115.
33. Rasmussen JA, Post DMB, Gibson BW, Lindemann SR, Apicella MA, Meyerholz DK, Jones BD. 2014. *Francisella tularensis* Schu S4 Lipopolysaccharide Core Sugar and O-Antigen Mutants Are Attenuated in a Mouse Model of Tularemia. *Infection and Immunity* 82:1523-1539.
34. Reed DS, Smith LP, Cole KS, Santiago AE, Mann BJ, Barry EM. 2014. Live attenuated mutants of *Francisella tularensis* protect rabbits against aerosol challenge with a virulent type A strain. *Infect Immun* 82:2098-105.
35. O'Malley KJ, Bowling JD, Stinson E, Cole KS, Mann BJ, Namjoshi P, Hazlett KRO, Barry EM, Reed DS. 2018. Aerosol prime-boost vaccination provides strong protection in outbred rabbits against virulent type A *Francisella tularensis*. *PLoS One* 13:e0205928.
36. Kirimanjeswara GS, Golden JM, Bakshi CS, Metzger DW. 2007. Prophylactic and Therapeutic Use of Antibodies for Protection against Respiratory Infection with *Francisella tularensis*. *The Journal of Immunology* 179:532-539.
37. Stenmark S, Lindgren H, Tärnvik A, Sjöstedt A. 2003. Specific antibodies contribute to the host protection against strains of *Francisella tularensis* subspecies *holarctica*. *Microbial Pathogenesis* 35:73-80.
38. Geier H, Celli J. 2011. Phagocytic receptors dictate phagosomal escape and intracellular proliferation of *Francisella tularensis*. *Infect Immun* 79:2204-14.
39. Chou AY, Kennett NJ, Melillo AA, Elkins KL. 2017. Murine survival of infection with *Francisella novicida* and protection against secondary challenge is critically dependent on B lymphocytes. *Microbes and Infection* 19:91-100.
40. Kilmury SL, Twine SM. 2010. The *Francisella tularensis* proteome and its recognition by antibodies. *Front Microbiol* 1:143.
41. Gaur R, Alam SI, Kamboj DV. 2017. Immunoproteomic Analysis of Antibody Response of Rabbit Host Against Heat-Killed *Francisella tularensis* Live Vaccine Strain. *Current Microbiology* 74:499-507.
42. Fulton KM, Zhao X, Petit MD, Kilmury SLN, Wolfraim LA, House RV, Sjöstedt A, Twine SM. 2011. Immunoproteomic analysis of the human antibody response to natural tularemia infection with Type A or Type B strains or LVS vaccination. *International Journal of Medical Microbiology* 301:591-601.
43. Savitt AG, Mena-Taboada P, Monsalve G, Benach JL. 2009. *Francisella tularensis* Infection-Derived Monoclonal Antibodies Provide Detection, Protection, and Therapy. *Clinical and Vaccine Immunology* 16:414-422.
44. Steiner DJ, Furuya Y, Metzger DW. 2018. Detrimental Influence of Alveolar Macrophages on Protective Humoral Immunity during *Francisella tularensis* SchuS4 Pulmonary Infection. *Infection and Immunity* 86:e00787-17.

45. Drabick JJ, Narayanan RB, Williams JC, Leduc JW, Nacy CA. 1994. Passive Protection of Mice Against Lethal *Francisella tularensis* (Live Tularemia Vaccine Strain) Infection by the Sera of Human Recipients of the Live Tularemia Vaccine. *The American Journal of the Medical Sciences* 308:83-87.
46. Fulop M, Mastroeni P, Green M, Titball RW. 2001. Role of antibody to lipopolysaccharide in protection against low- and high-virulence strains of *Francisella tularensis*. *Vaccine* 19:4465-4472.
47. Francis E, Felton LD. 1942. Antitularemic Serum. *Public Health Reports (1896-1970)* 57:44-55.
48. Pannell L, Cordle MS. 1962. Further Studies on Protective Filtrates of *Pasteurella tularensis* Broth Cultures. *The Journal of Infectious Diseases* 111:49-54.
49. Allen WP. 1962. Immunity Against Tularemia: Passive Protection of Mice by Transfer of Immune Tissues. *The Journal of Experimental Medicine* 115:411-420.
50. Mara-Koosham G, Hutt JA, Lyons CR, Wu TH. 2011. Antibodies contribute to effective vaccination against respiratory infection by type A *Francisella tularensis* strains. *Infect Immun* 79:1770-8.
51. Stinson E, Smith LP, Cole KS, Barry EM, Reed DS. 2016. Respiratory and oral vaccination improves protection conferred by the live vaccine strain against pneumonic tularemia in the rabbit model. *Pathog Dis* 74.
52. Glynn AR, Alves DA, Frick O, Erwin-Cohen R, Porter A, Norris S, Waag D, Nalca A. 2015. Comparison of experimental respiratory tularemia in three nonhuman primate species. *Comparative Immunology, Microbiology and Infectious Diseases* 39:13-24.
53. Hutt JA, Lovchik JA, Dekonenko A, Hahn AC, Wu TH. 2017. The Natural History of Pneumonic Tularemia in Female Fischer 344 Rats after Inhalational Exposure to Aerosolized *Francisella tularensis* Subspecies *tularensis* Strain SCHU S4. *The American Journal of Pathology* 187:252-267.
54. Grey MR, Spaeth KR. 2006. Chapter 16. Tularemia (*Francisella tularensis*), *The Bioterrorism Sourcebook*. The McGraw-Hill Companies, New York, NY.
55. Petersen JM, Dennis DT, Beard CB. 2017. 127 - Tularemia, p 1085-1090.e1. *In* Cohen J, Powderly WG, Opal SM (ed), *Infectious Diseases (Fourth Edition)* doi:<https://doi.org/10.1016/B978-0-7020-6285-8.00127-1>. Elsevier.
56. Hepburn MJ, Simpson AJ. 2008. Tularemia: current diagnosis and treatment options. *Expert review of anti-infective therapy* 6:231-240.
57. Page M, Thorpe R. 2002. Purification of IgG Using Caprylic Acid, p 985-985. *In* Walker JM (ed), *The Protein Protocols Handbook* doi:10.1385/1-59259-169-8:985. Humana Press, Totowa, NJ.
58. Page M, Thorpe R. 2002. Purification of IgG by Precipitation with Sodium Sulfate or Ammonium Sulfate, p 983-984. *In* Walker JM (ed), *The Protein Protocols Handbook* doi:10.1385/1-59259-169-8:983. Humana Press, Totowa, NJ.
59. Bio-Rad Laboratories I. General Protocol: SDS-PAGE, p 60, *Electrophoresis Guide*.
60. Anonymous. 2006. Coomassie Brilliant Blue solution. *Cold Spring Harbor Protocols* 2006:pdb.rec9077.
61. Smith PK, Krohn RI, Hermanson GT, Mallia AK, Gartner FH, Provenzano MD, Fujimoto EK, Goeke NM, Olson BJ, Klenk DC. 1985. Measurement of protein using bicinchoninic acid. *Analytical Biochemistry* 150:76-85.

62. Faith SA, Smith LP, Swatland AS, Reed DS. 2012. Growth conditions and environmental factors impact aerosolization but not virulence of *Francisella tularensis* infection in mice. *Front Cell Infect Microbiol* 2:126.
63. Guyton AC. 1947. Measurement of the Respiratory Volumes of Laboratory Animals. *American Journal of Physiology-Legacy Content* 150:70-77.
64. McQuillen DP, Gulati S, Rice PA. 1994. Complement-mediated bacterial killing assays, p 137-147, *Methods in Enzymology*, vol 236. Academic Press.
65. Sato T, Fujita H, Ohara Y, Homma M. 1990. Microagglutination test for early and specific serodiagnosis of tularemia. *J Clin Microbiol* 28:2372-4.
66. Gaultney JB, Wende RD, Williams RP. 1971. Microagglutination procedures for febrile agglutination tests. *Applied microbiology* 22:635-640.
67. Ben Nasr A, Klimpel GR. 2008. Subversion of complement activation at the bacterial surface promotes serum resistance and opsonophagocytosis of *Francisella tularensis*. *Journal of leukocyte biology* 84:77-85.
68. Hrstka R, Stulík J, Vojtěšek B. 2005. The role of MAPK signal pathways during *Francisella tularensis* LVS infection-induced apoptosis in murine macrophages. *Microbes and Infection* 7:619-625.
69. Trivedi NH, Yu JJ, Hung CY, Doelger RP, Navara CS, Armitige LY, Seshu J, Sinai AP, Chambers JP, Guentzel MN, Arulanandam BP. 2018. Microbial co-infection alters macrophage polarization, phagosomal escape, and microbial killing. *Innate Immun* 24:152-162.
70. Holicka M, Novosad J, Kudlova M, Loudova M, Andrys C, Krejsek J. 2010. J774 macrophage-like cell line cytokine and chemokine patterns are modulated by *Francisella tularensis* LVS strain infection. *Folia Microbiologica* 55:191-200.
71. Mara-Koosham G, Hutt JA, Lyons CR, Wu TH. 2011. Antibodies Contribute to Effective Vaccination against Respiratory Infection by Type A *Francisella tularensis* Strains. *Infection and Immunity* 79:1770-1778.